SAND2008-2606C

Elastic Wave Radiation From A Resonating Line Source

David F. Aldridge, Leiph A. Preston,
Nathan E. Gaunt, and Neill P. Symons

Geophysics Department
Sandia National Laboratories
Albuquerque, New Mexico, USA

Seismological Society of America 2008 Annual Meeting
Santa Fe, New Mexico
16-18 April 2008

Elastodynamic Velocity-Stress System

$$\frac{\partial v_i}{\partial t} - \frac{1}{\rho}\frac{\partial \sigma_{ij}}{\partial x_j} = \frac{1}{\rho}\left[f_i + \frac{\partial m_{ij}^a}{\partial x_j} \right] \qquad \text{(3 equations)}$$

$$\frac{\partial \sigma_{ij}}{\partial t} - \lambda \frac{\partial v_k}{\partial x_k}\delta_{ij} - \mu\left[\frac{\partial v_i}{\partial x_j} + \frac{\partial v_j}{\partial x_i} \right] = \frac{\partial m_{ij}^s}{\partial t} \qquad \text{(6 equations)}$$

Nine, coupled, first-order, linear, non-homogeneous partial differential equations.

Wavefield variables:
- $v_i(\mathbf{x},t)$ - velocity vector
- $\sigma_{ij}(\mathbf{x},t)$ - stress tensor

Earth model parameters:
- $\rho(\mathbf{x})$ - mass density
- $\lambda(\mathbf{x})$, $\mu(\mathbf{x})$ - elastic moduli

Body sources:
- $f_i(\mathbf{x},t)$ - force vector
- $m_{ij}(\mathbf{x},t)$ - moment tensor

Derived from fundamental principles of continuum mechanics (conservation of mass, balance of linear and angular momentum), an isotropic elastic stress-strain constitutive relation, and linearization to the infinitesimal deformation regime.

Staggered Spatial and Temporal FD Schemes

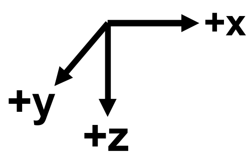

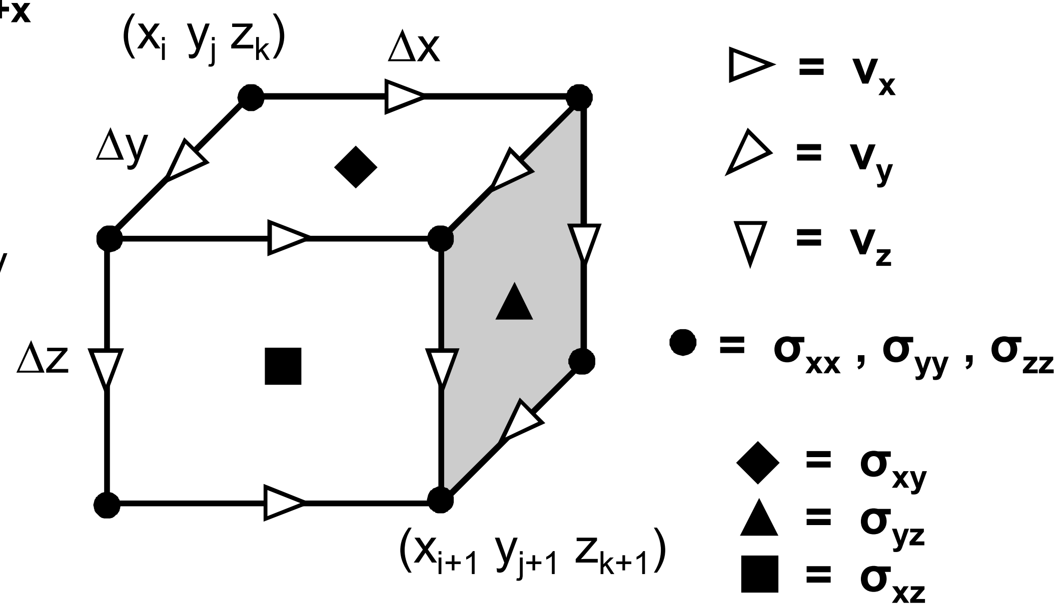

3D spatial staggering
⇒ high centered FD operator accuracy

1D temporal staggering
⇒ high centered FD operator accuracy

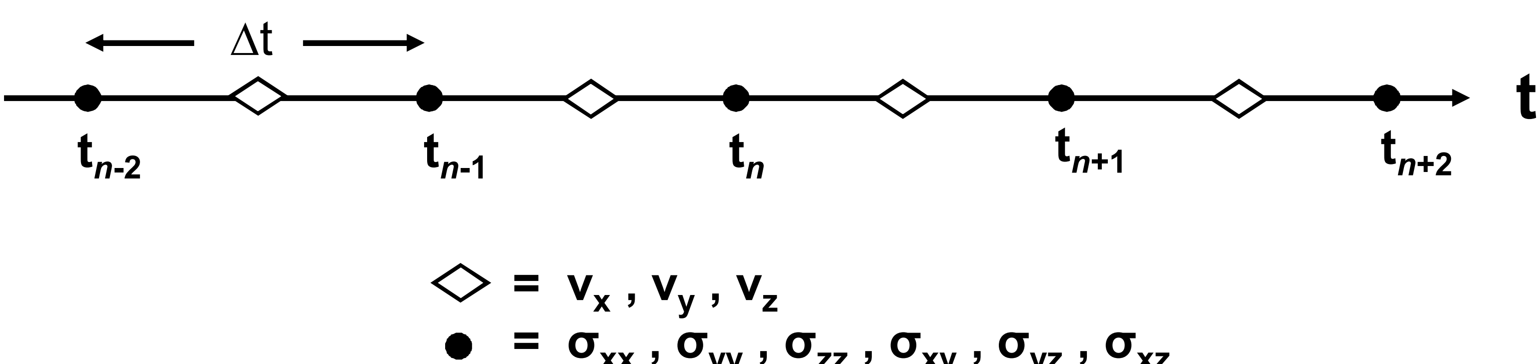

Straight Air-Filled Tunnel Model

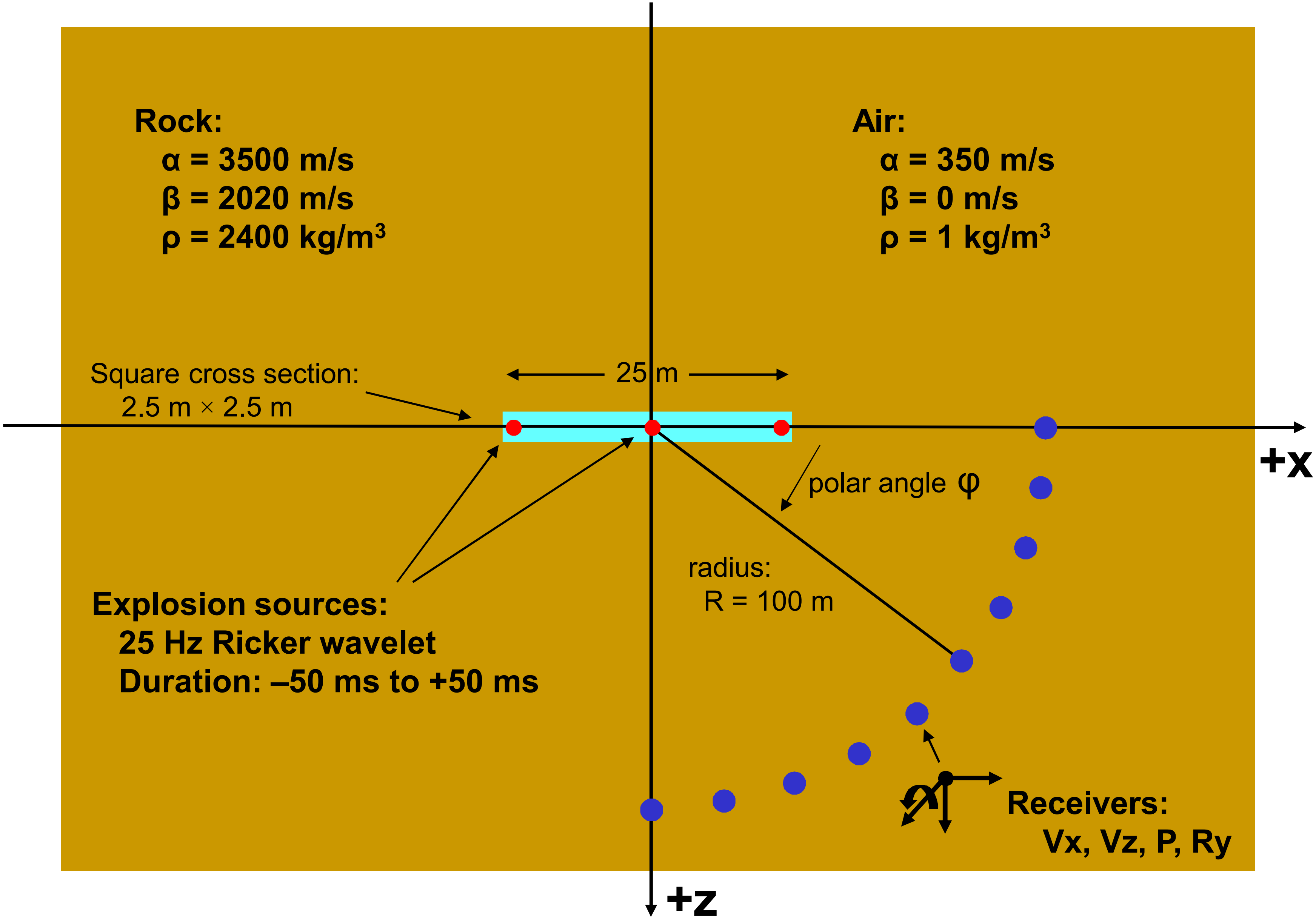

Finite-Difference Modeling Specifications

3D wave propagation modeling with an O(2,2) staggered-grid FD algorithm for isotropic elastic media:

1) Earth Model:

1.1) background: homogeneous wholespace (no free surface) with
α = 3500 m/s, β = 2020 m/s, ρ = 2400 kg/m^3.

1.2) tunnel: square cross-section with 2.5 m x 2.5m x 25 m dimensions;
α = 350 m/s, β = 0 m/s, ρ = 1 kg/m^3.

2) Numerical Grids:

2.1) Spatial: $\Delta x = \Delta y = \Delta z$ = 0.5 m; 501 x 501 x 501 ~ 125 million gridpoints;
~6.04 Gbytes RAM required (for 12 3D single-precision arrays).

2.2) Temporal: Δt = 0.070 ms; 10716 timesteps; simulation time 750 ms.

3) Acquisition Parameters:

2.1) Point isotropic explosion at (0, 0, 0) m (center of tunnel) and (-12,0,0) m (left end of tunnel); 25 Hz Ricker wavelet, duration –50 ms to + 50 ms.

2.2) Timeslices capturing Vz, Vx, P, and Ry on an xz plane through source location.

2.3) Point receivers recording Vz, Vx, P, and Wy at 100 m radius from tunnel center.

4) Computation:

4.1) Single processor workstation with Intel Xeon 5160; 3 GHz rate, 4 Mbyte cache.

4.3) 64 bit addressing required to access sufficient RAM.

4.2) Execution time: 2126 minutes = 35.4 hours = 1.48 days.

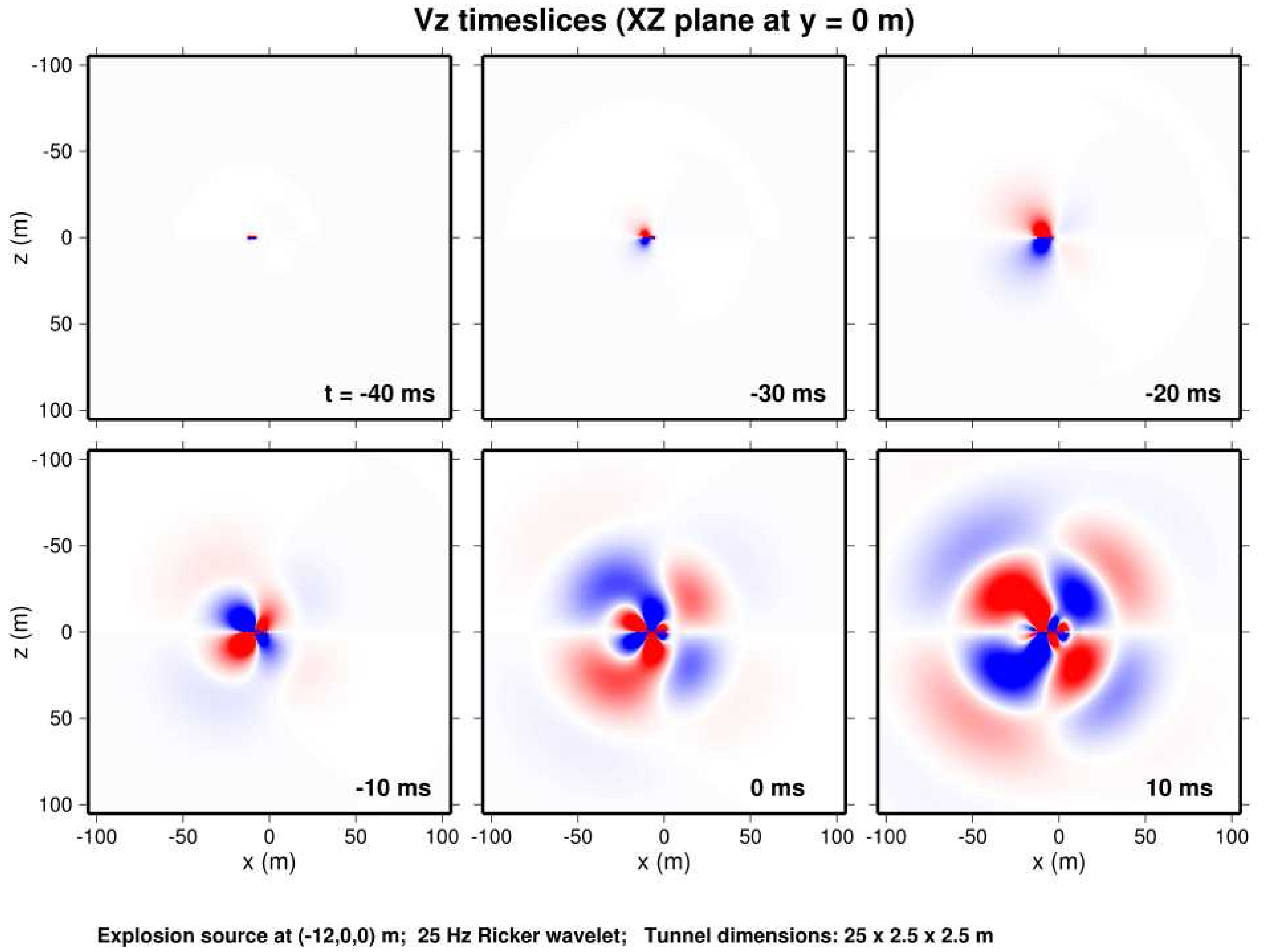
Vz timeslices (XZ plane at y = 0 m)
t = -40 ms
-30 ms
-20 ms
-10 ms
0 ms
10 ms
z (m)
x (m)
-100
-50
0
50
100
Explosion source at (-12,0,0) m; 25 Hz Ricker wavelet; Tunnel dimensions: 25 x 2.5 x 2.5 m

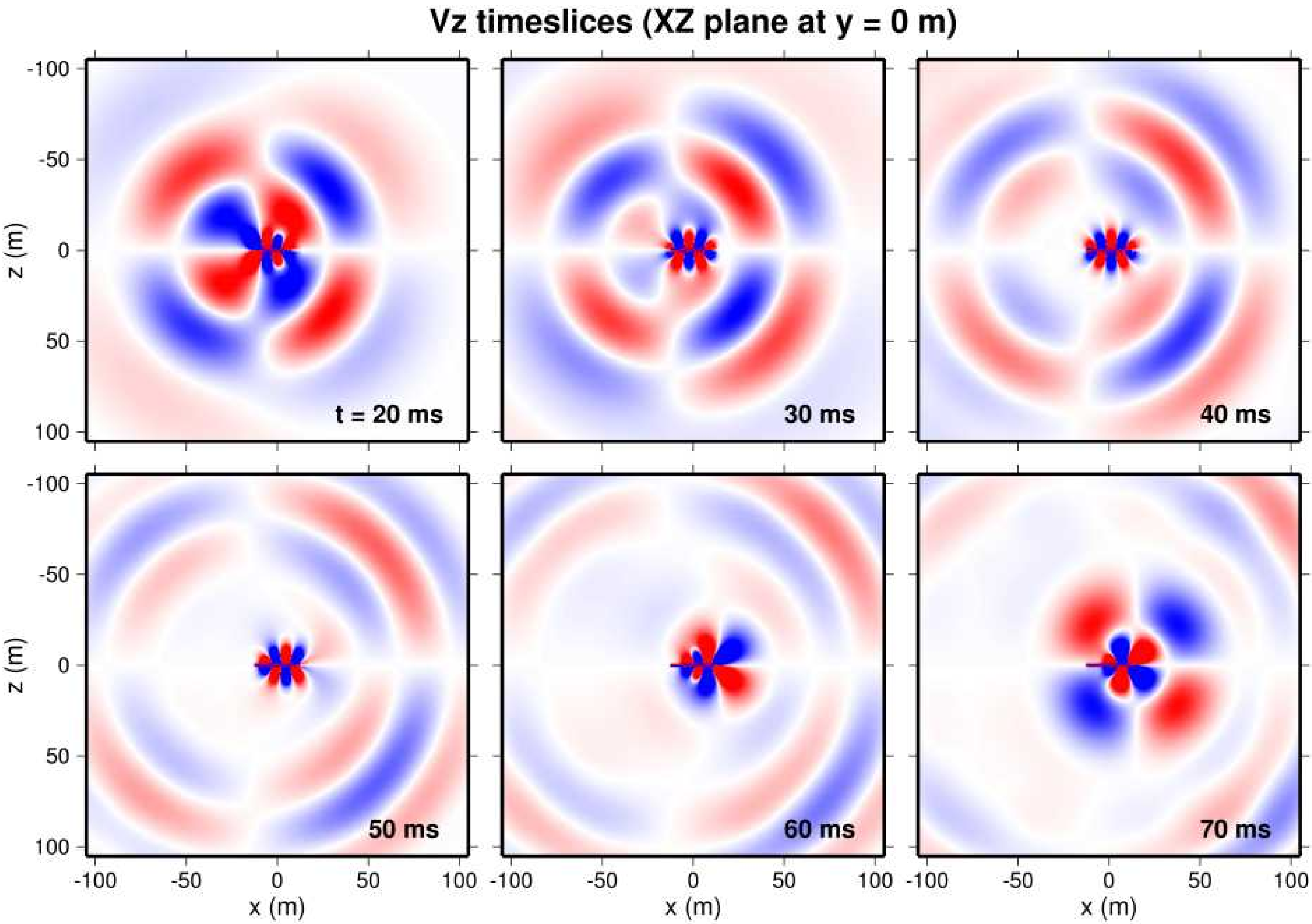

Explosion source at (-12,0,0) m; 25 Hz Ricker wavelet; Tunnel dimensions: 25 x 2.5 x 2.5 m

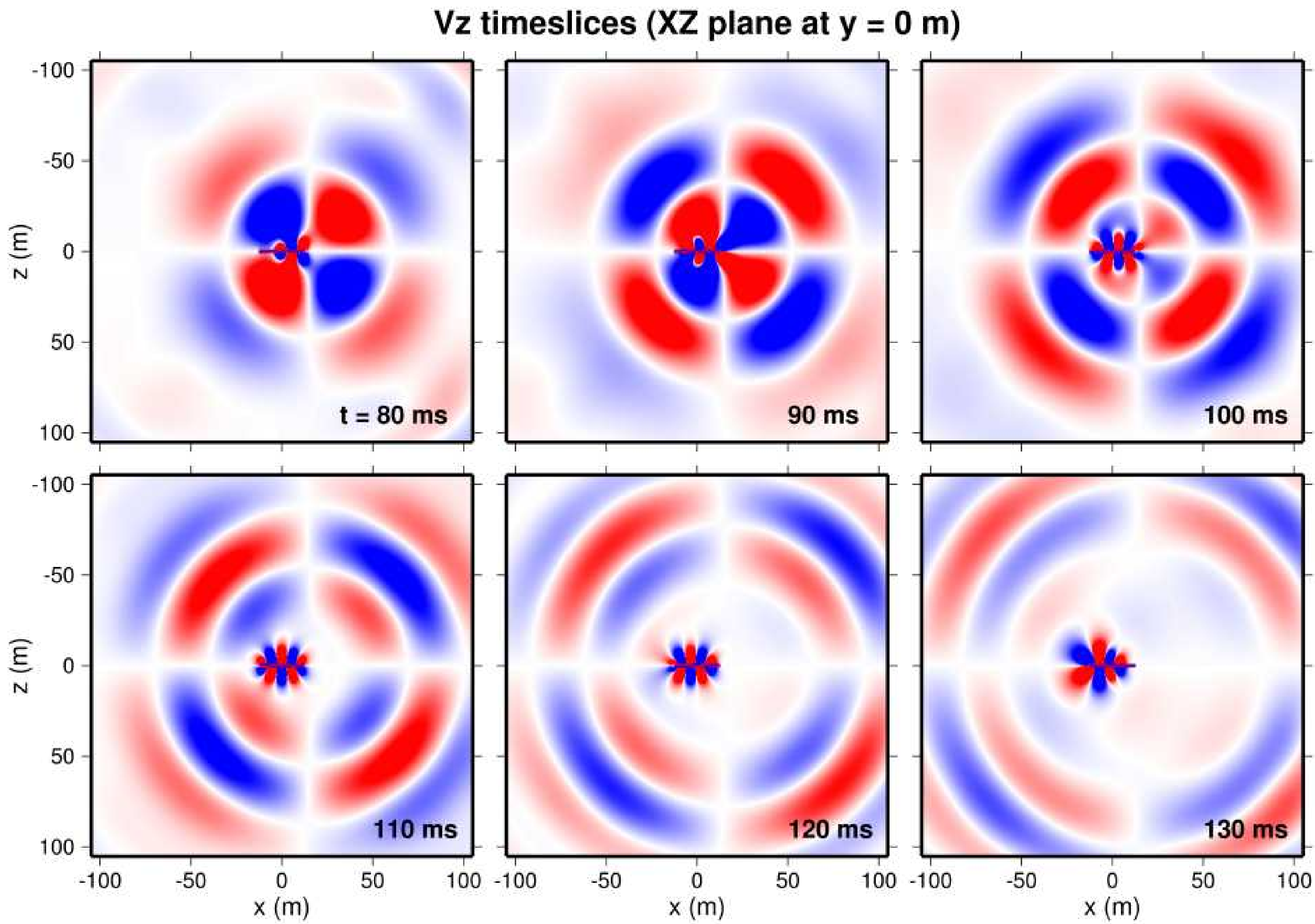

Explosion source at (-12,0,0) m; 25 Hz Ricker wavelet; Tunnel dimensions: 25 x 2.5 x 2.5 m

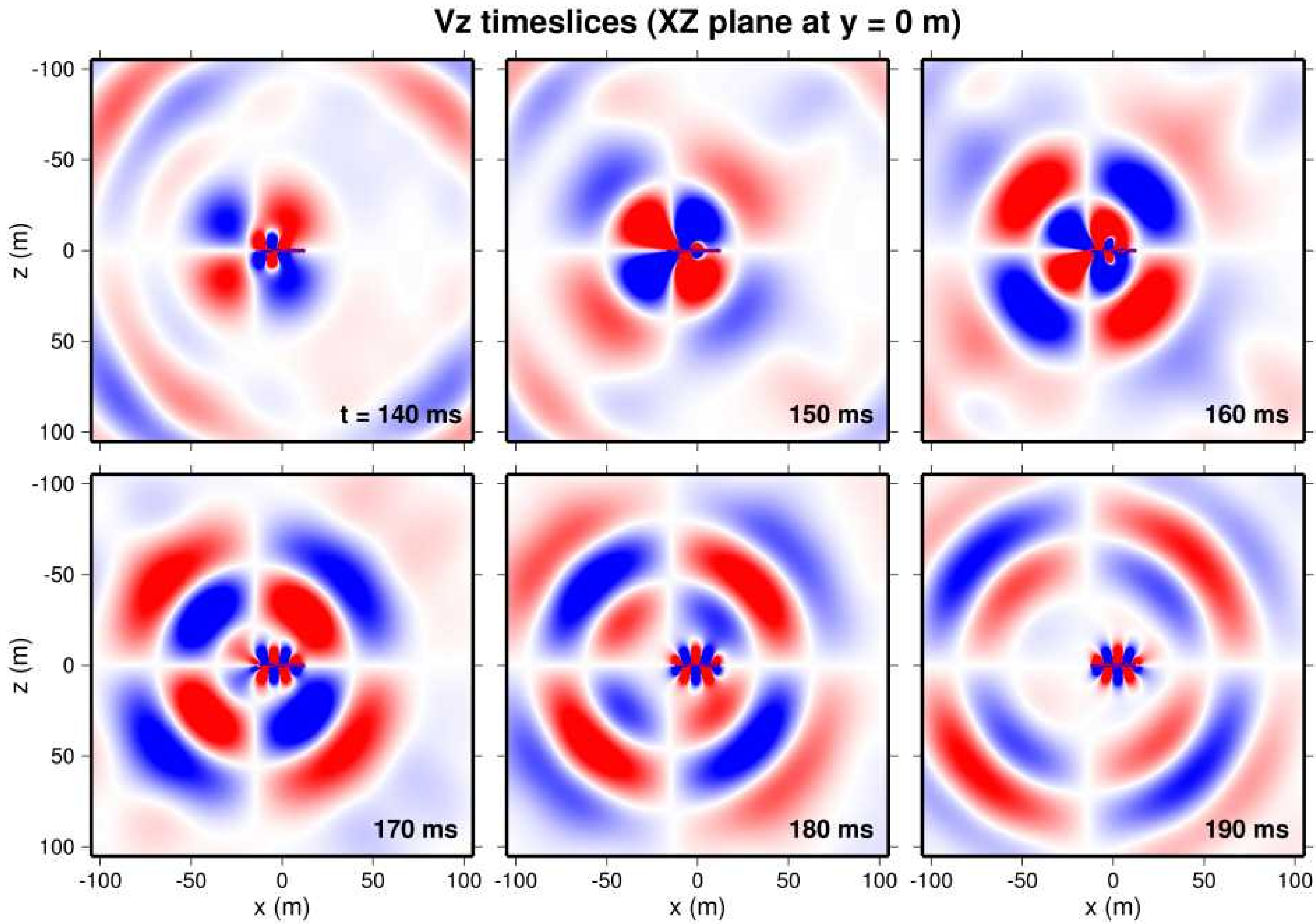

Explosion source at (-12,0,0) m; 25 Hz Ricker wavelet; Tunnel dimensions: 25 x 2.5 x 2.5 m

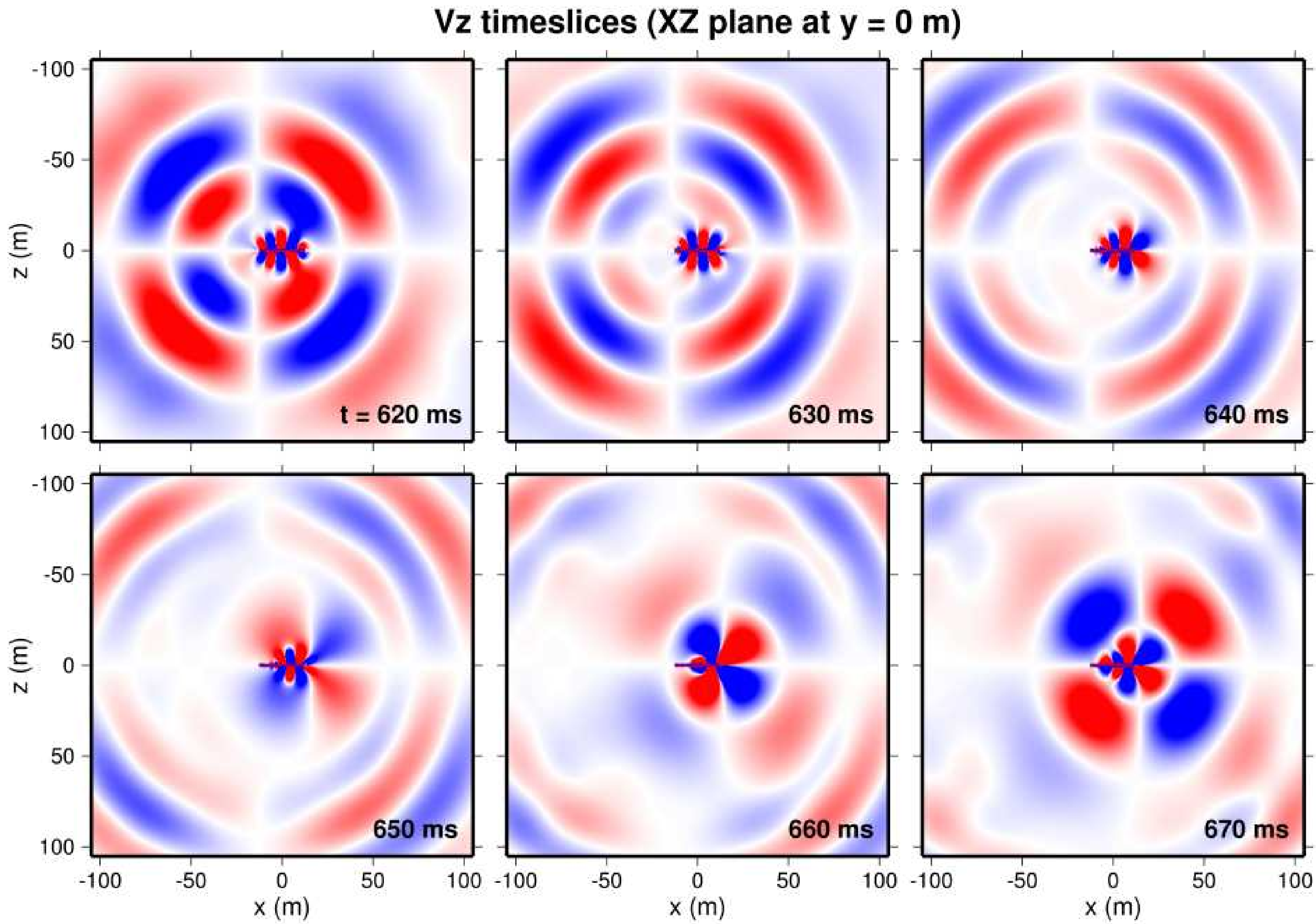

Explosion source at (-12,0,0) m; 25 Hz Ricker wavelet; Tunnel dimensions: 25 x 2.5 x 2.5 m

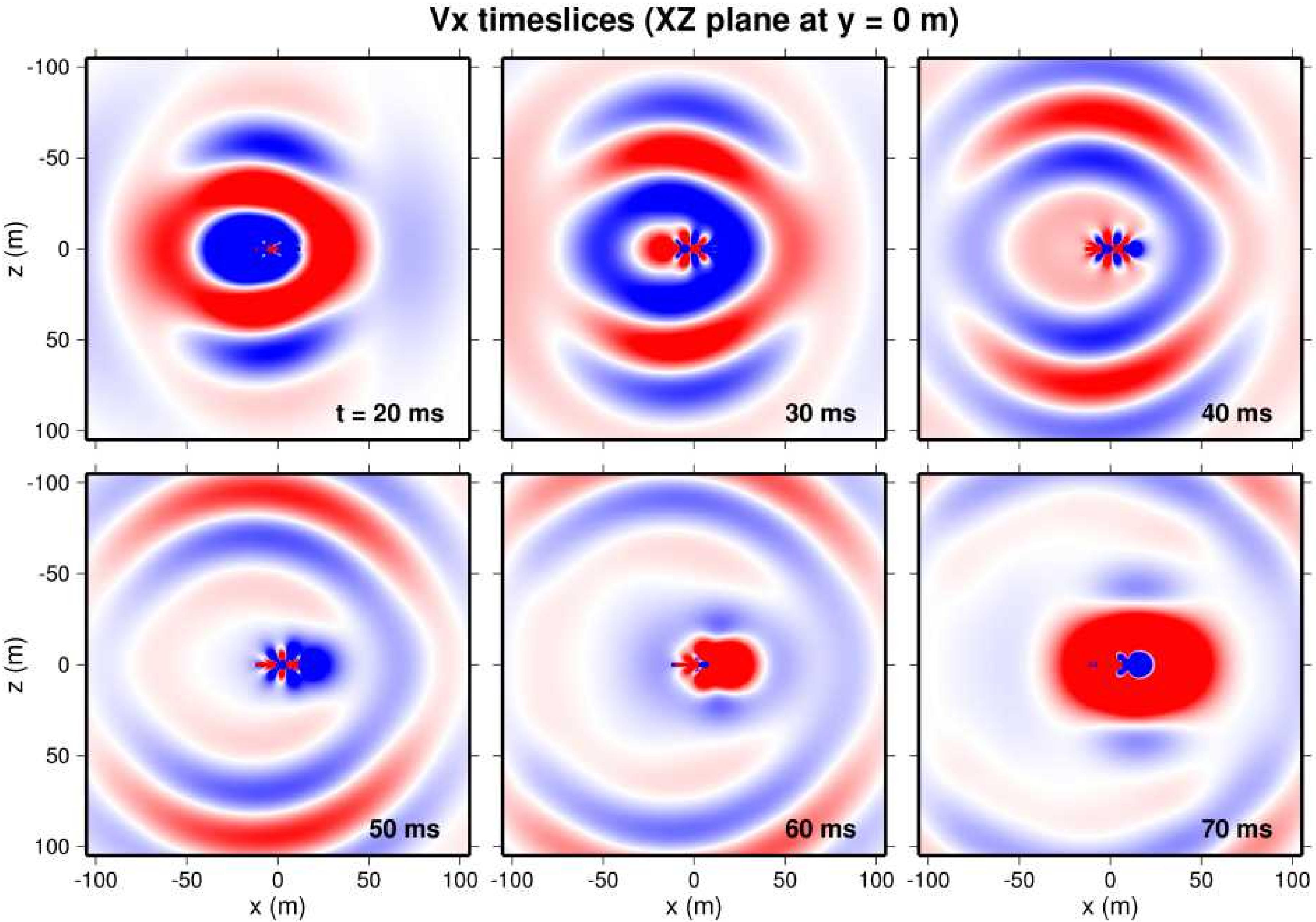

Explosion source at (-12,0,0) m; 25 Hz Ricker wavelet; Tunnel dimensions: 25 x 2.5 x 2.5 m

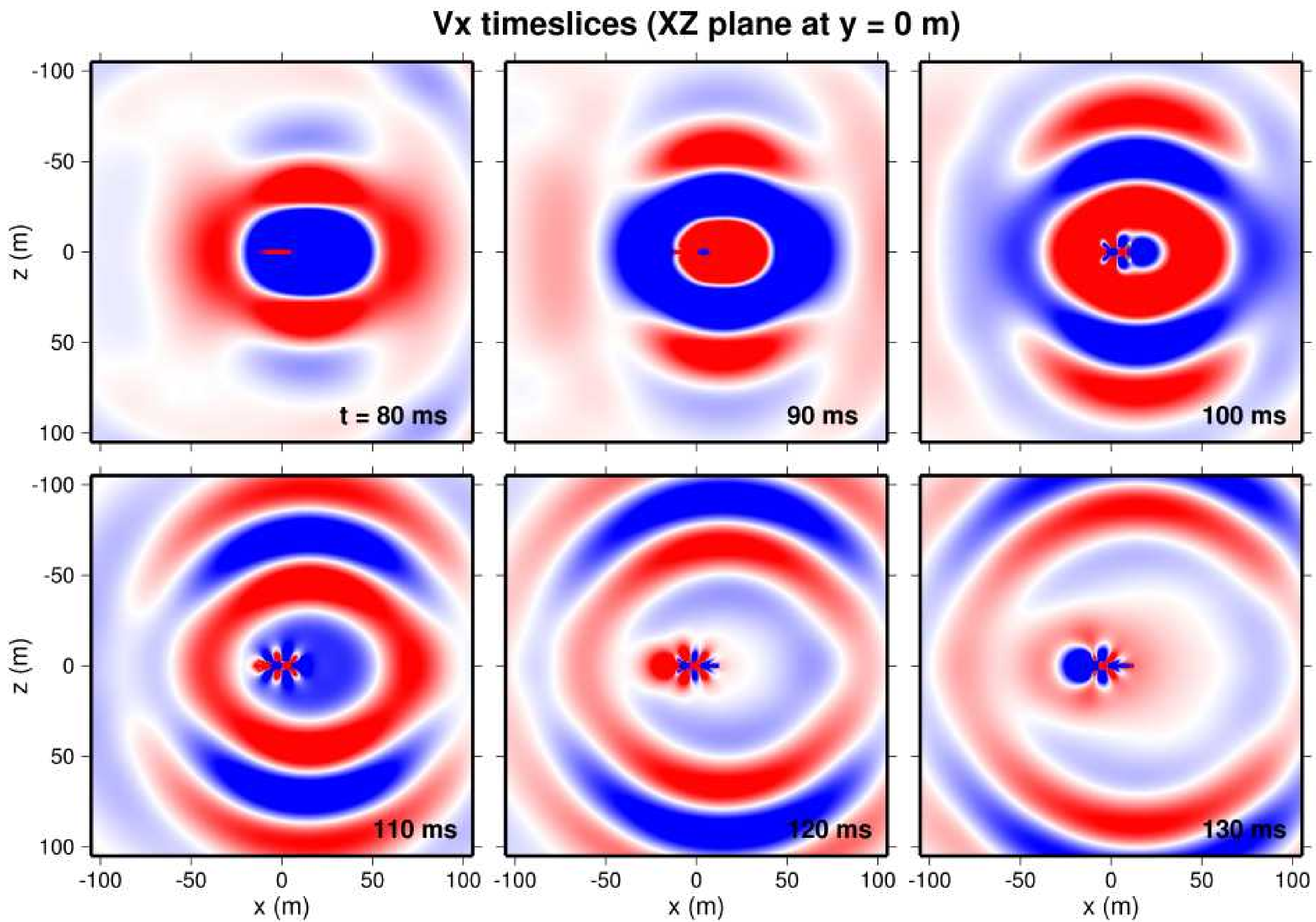

Explosion source at (-12,0,0) m; 25 Hz Ricker wavelet; Tunnel dimensions: 25 x 2.5 x 2.5 m

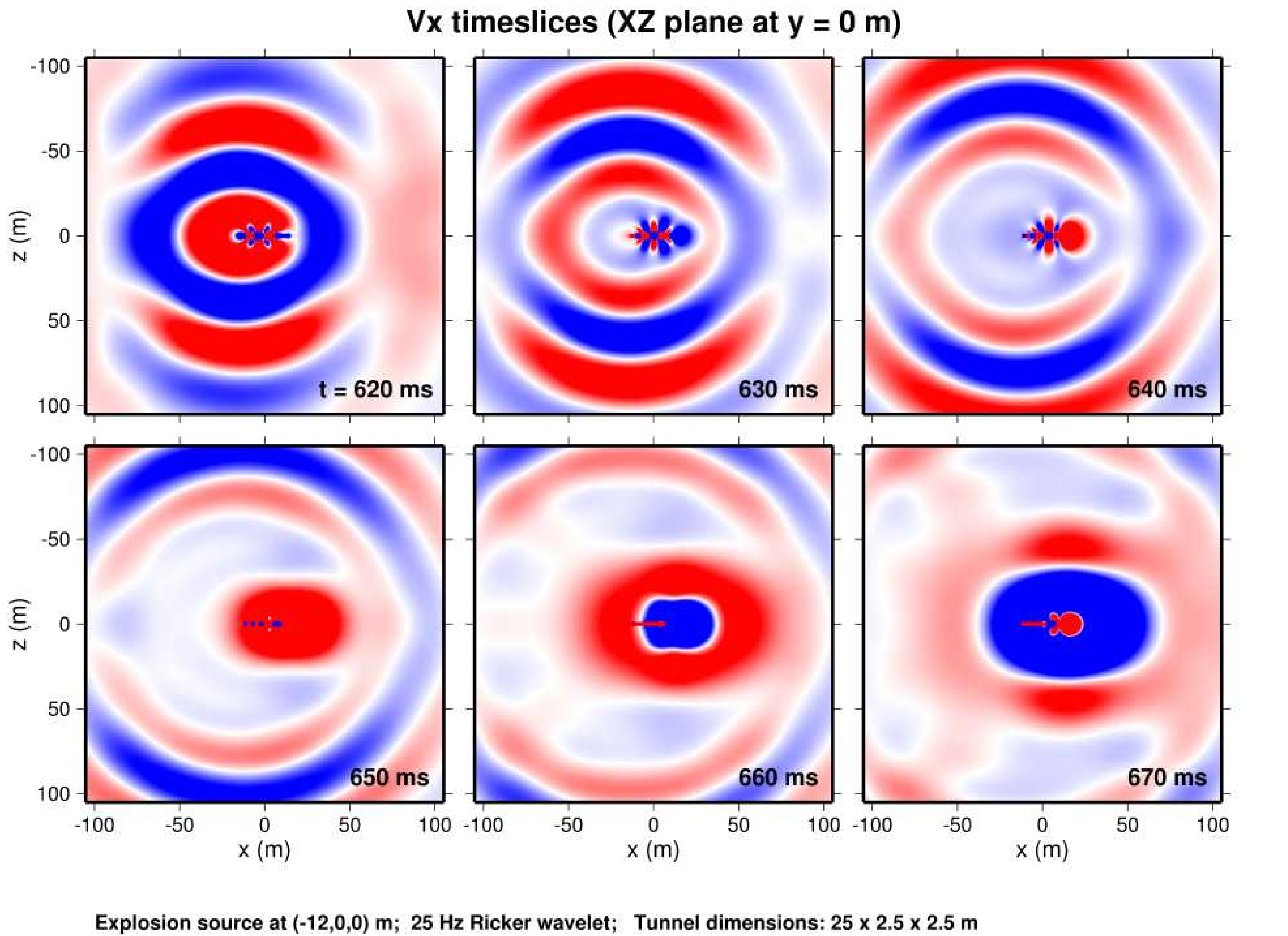
Vx timeslices (XZ plane at y = 0 m)
-100
-50
0
50
100
z (m)
t = 620 ms
630 ms
640 ms
650 ms
660 ms
670 ms
-100
-50
0
50
100
x (m)
Explosion source at (-12,0,0) m; 25 Hz Ricker wavelet;   Tunnel dimensions: 25 x 2.5 x 2.5 m

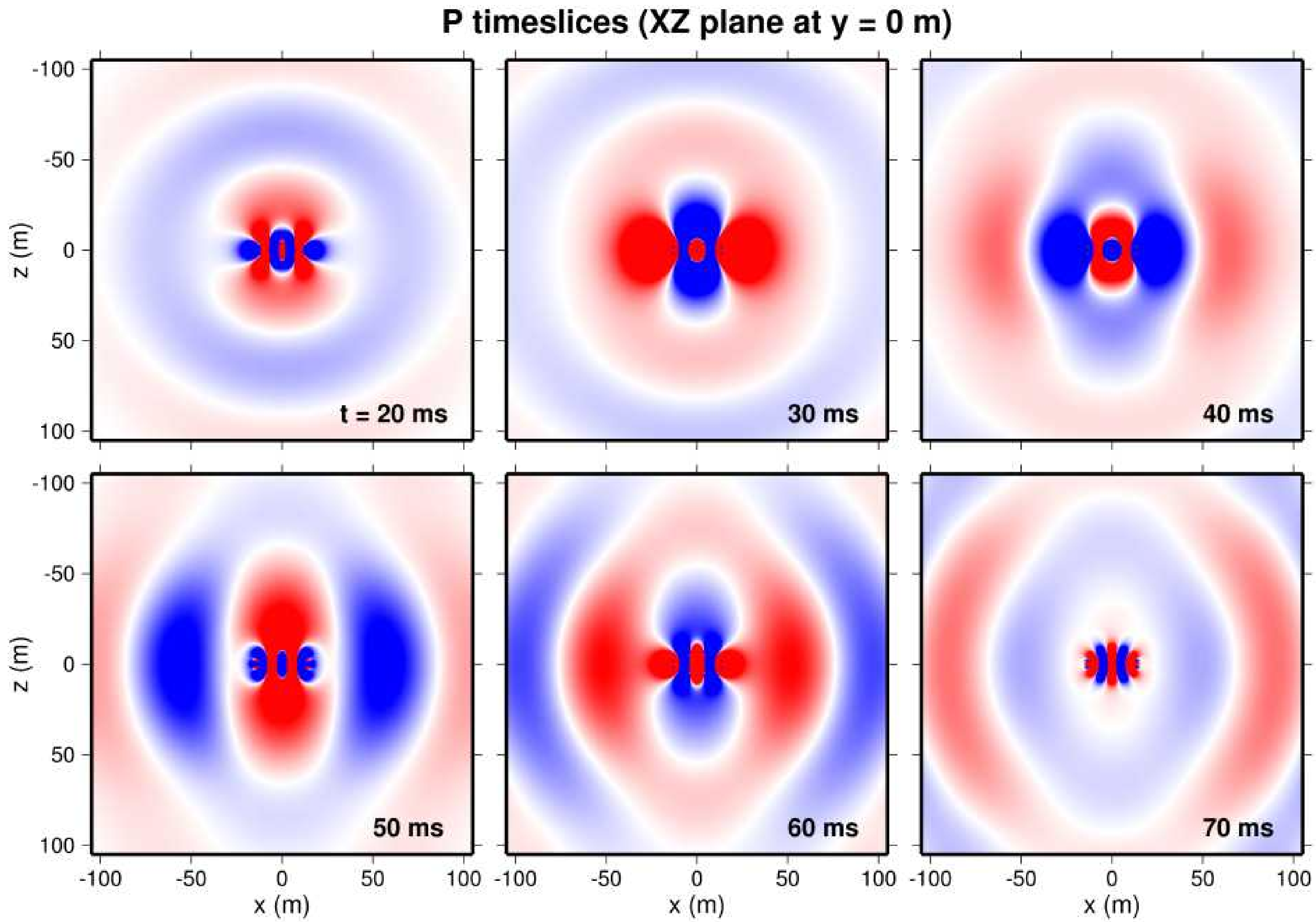

Explosion source at (0,0,0) m; 25 Hz Ricker wavelet; Tunnel dimensions: 25 x 2.5 x 2.5 m

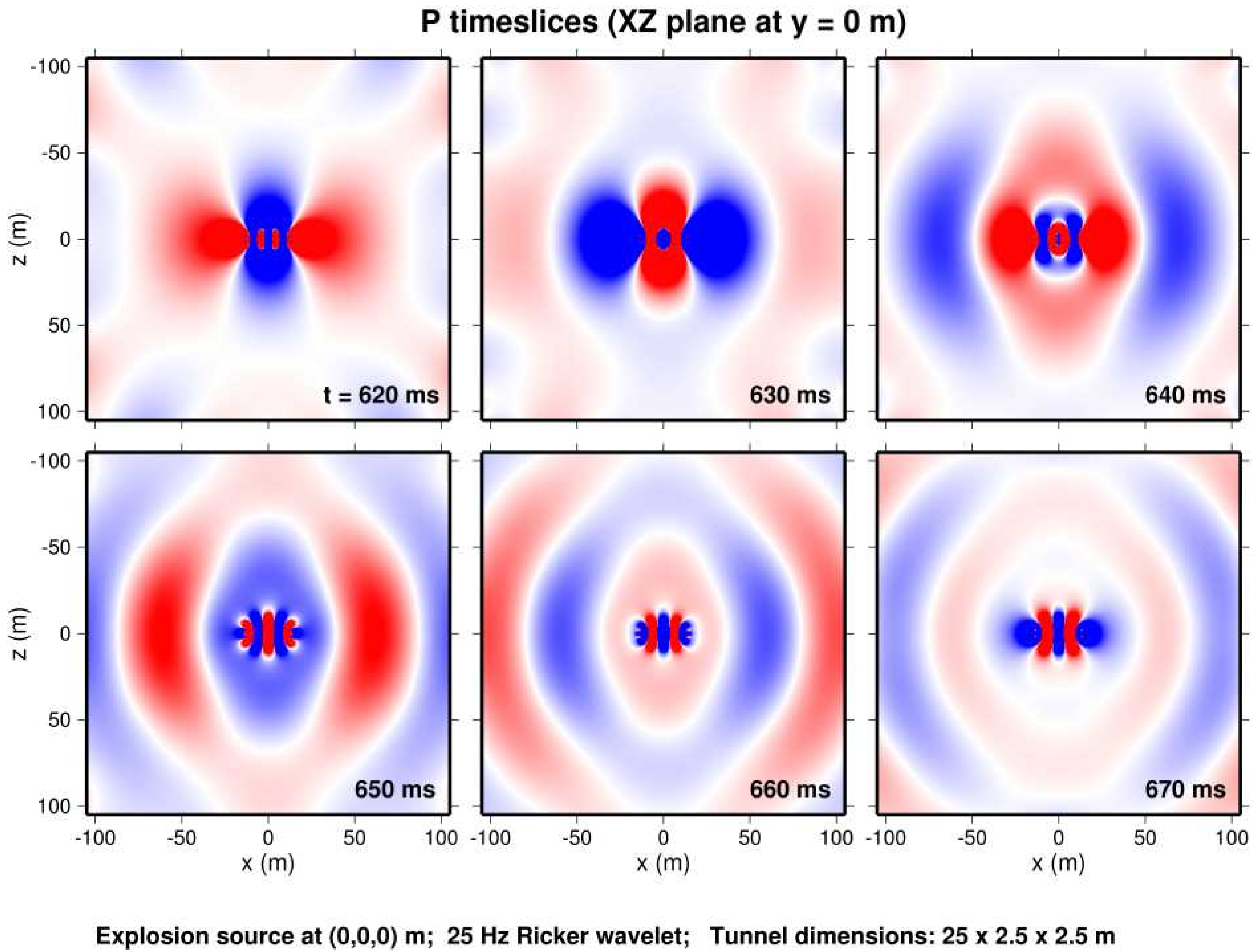
P timeslices (XZ plane at y = 0 m)
t = 620 ms
630 ms
640 ms
650 ms
660 ms
670 ms
z (m)
x (m)
-100
-50
0
50
100
Explosion source at (0,0,0) m; 25 Hz Ricker wavelet;   Tunnel dimensions: 25 x 2.5 x 2.5 m

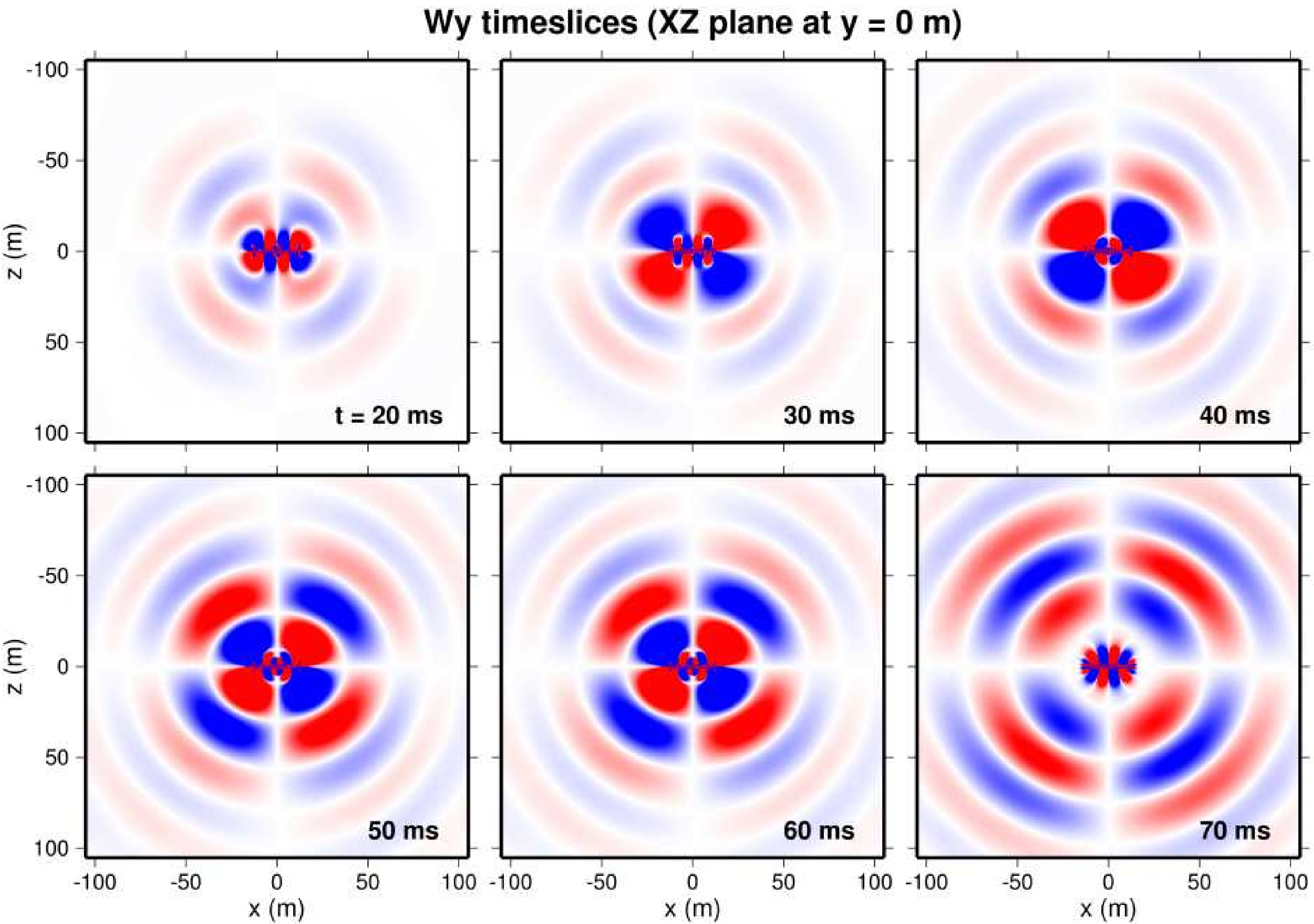

Explosion source at (0,0,0) m; 25 Hz Ricker wavelet; Tunnel dimensions: 25 x 2.5 x 2.5 m

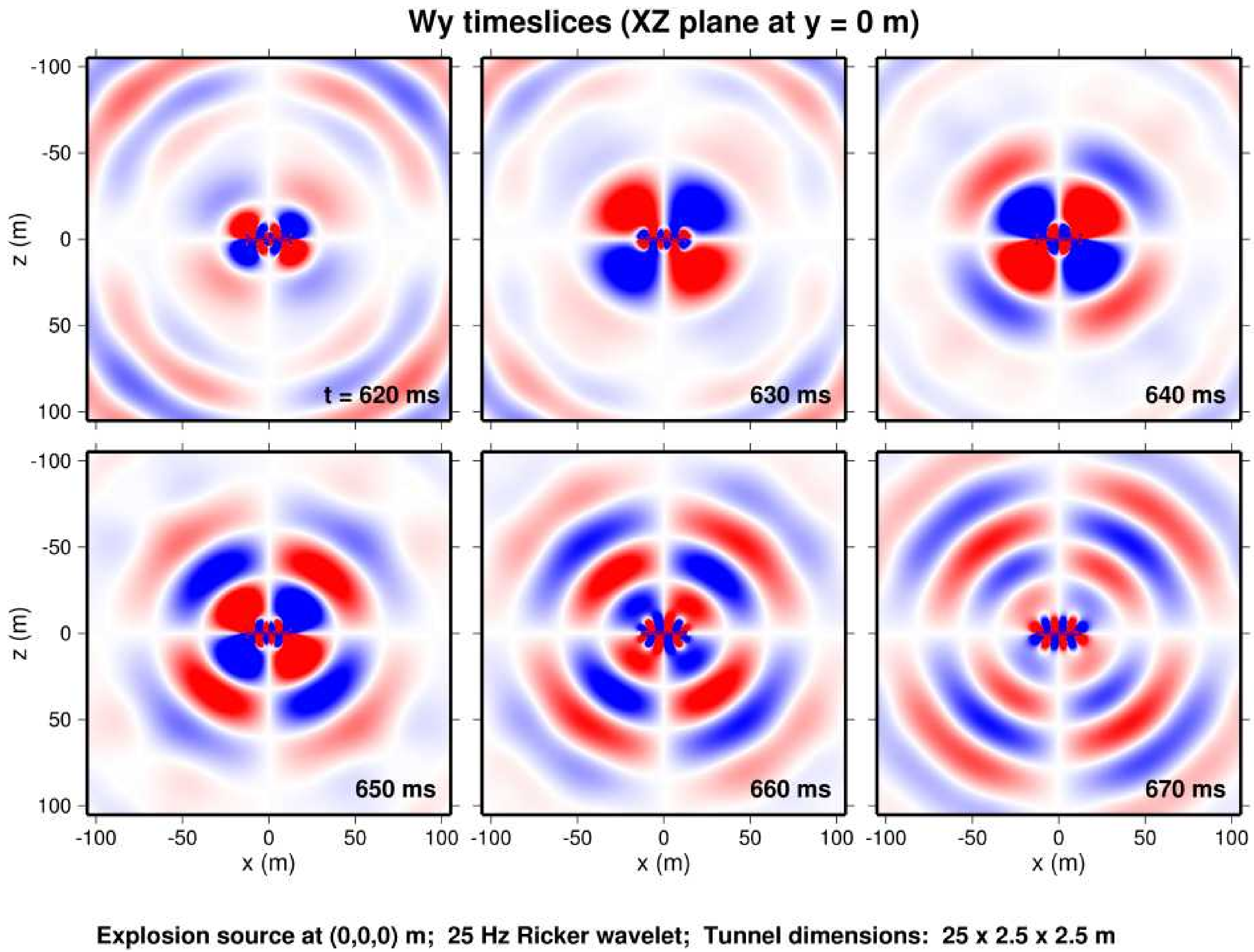
Wy timeslices (XZ plane at y = 0 m)
t = 620 ms
630 ms
640 ms
650 ms
660 ms
670 ms
z (m)
x (m)
-100
-50
0
50
100
Explosion source at (0,0,0) m; 25 Hz Ricker wavelet; Tunnel dimensions: 25 x 2.5 x 2.5 m

Resonant Response Comparison (Vz, Vx, P, Ry)

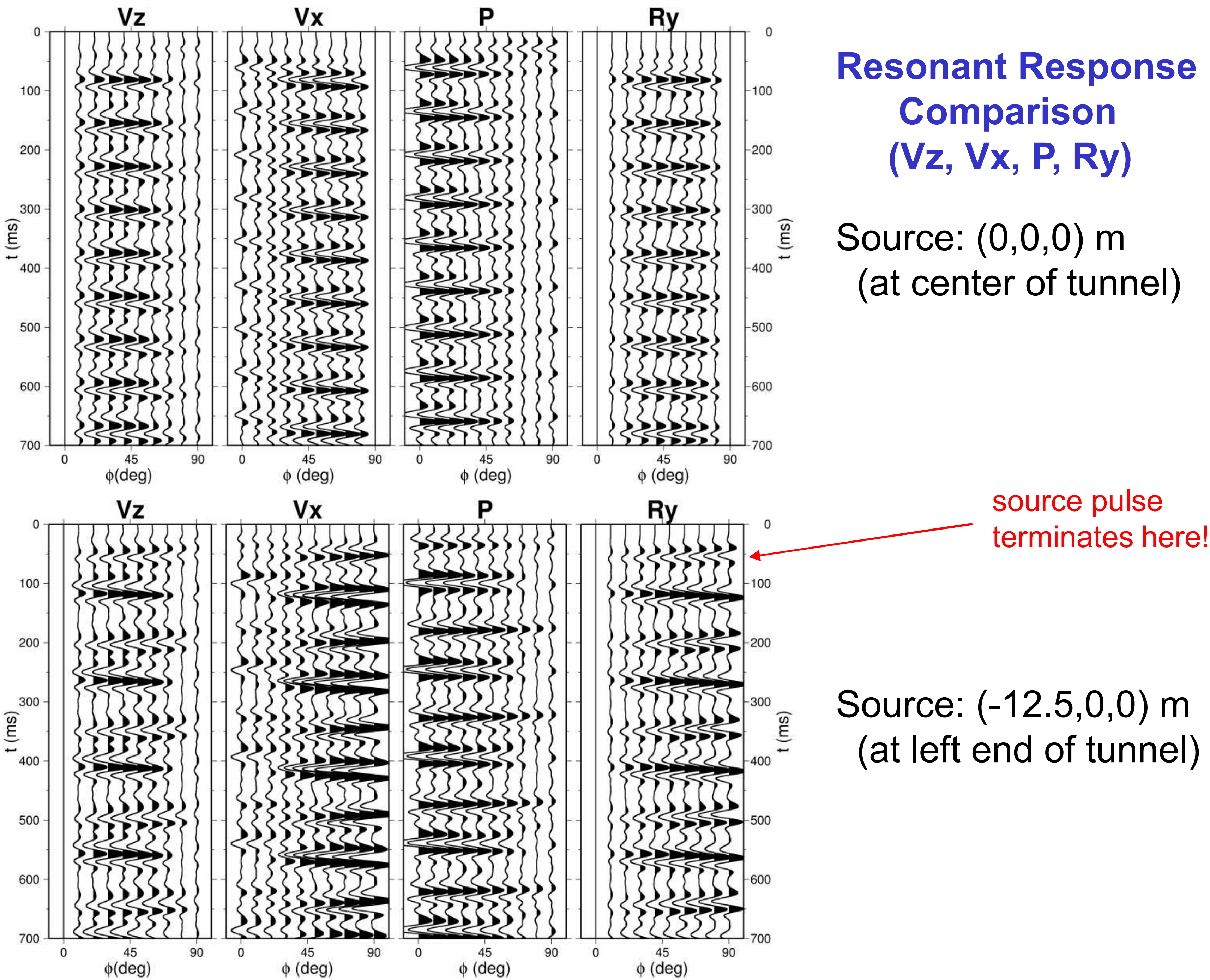

Source: (0,0,0) m
(at center of tunnel)

Source: (-12.5,0,0) m
(at left end of tunnel)

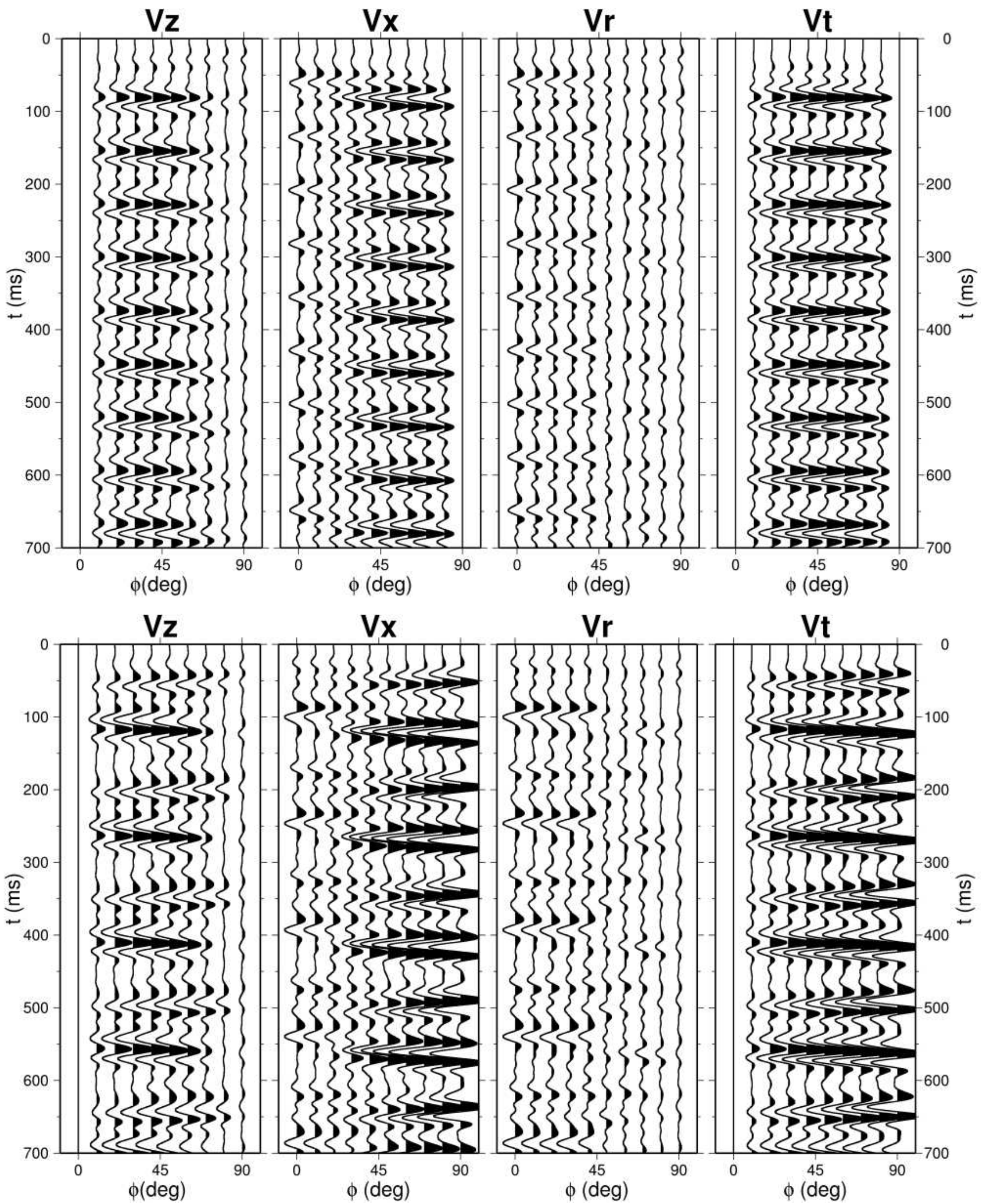

Resonant Response Comparison (Vz, Vx, Vr, Vt)

Source: (0,0,0) m
(at center of tunnel)

Source: (-12.5,0,0) m
(at left end of tunnel)

The Seismological Model

Homogeneous and isotropic elastic wholespace:

P-wave speed: α
S-wave speed: β
Mass density: ρ

An infinitely-long, evacuated, cylindrical borehole of radius a

Time-varying traction applied to finite-length h of borehole wall:

1) radial: +r direction
2) axial: +z direction
3) tangential: +θ direction

Cylindrical (r,θ,z) coordinate system parameterization:

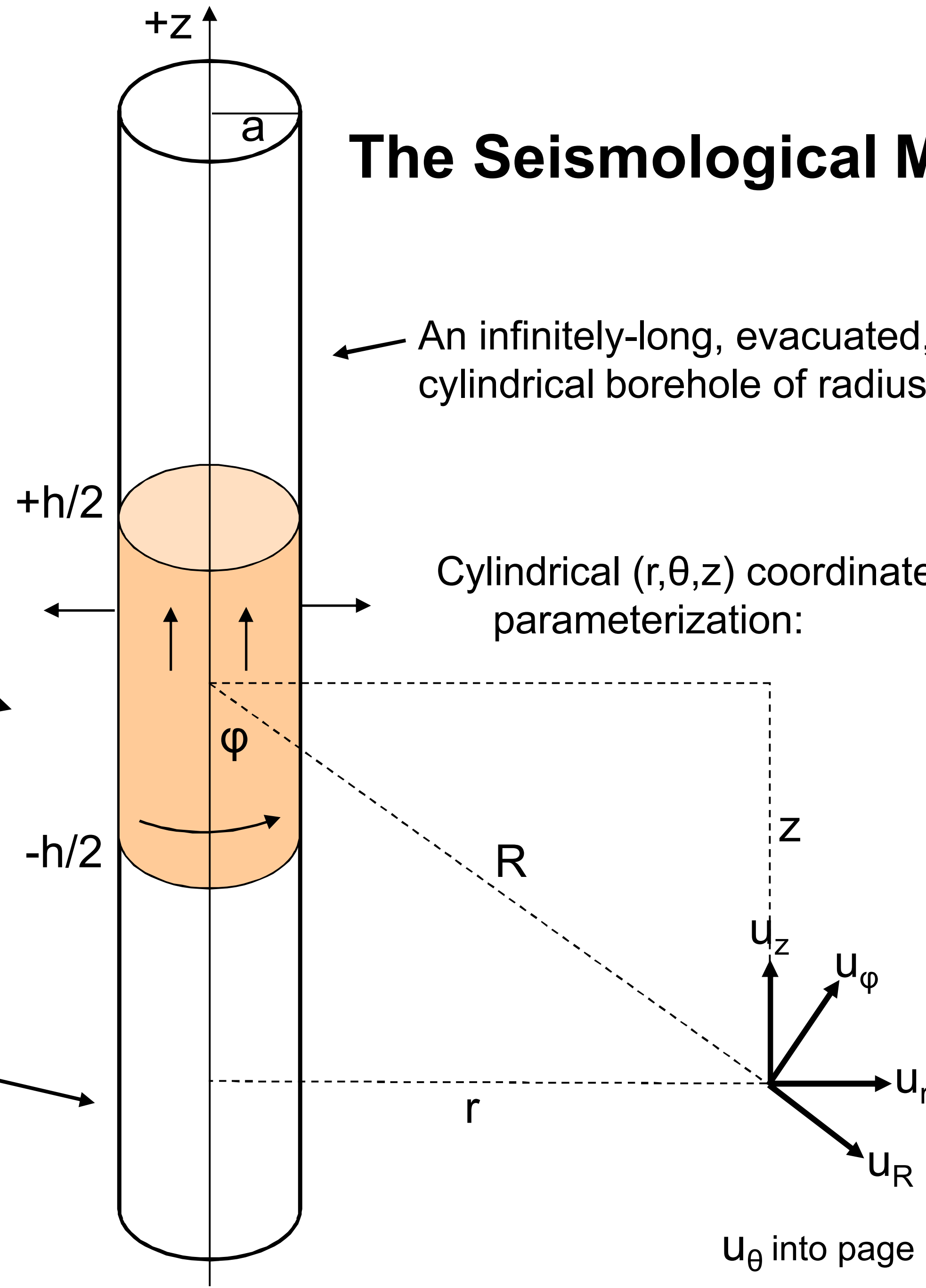

Stress vanishes elsewhere on borehole wall

Traveling, Axi-Symmetric, Radial Stress Pulse

stress wavelet

time/space positioning parameters

$$s_r(z,t) = S\,\Pi\left(\frac{z}{h}\right) w\left(t - t_0 - \frac{z - z_0}{v}\right)$$

rectangle function localizes stress to –h/2 < z < +h/2

pulse propagation speed

A better pulse? : $\Pi\left(\frac{z}{h}\right)\exp\left[-\kappa\left(z - z_0\right)\right] w\left(t - t_0 - \frac{z - z_0}{v}\right)$

Far-Field (1/R) Particle Velocity Solution

Far-field radial velocity:

$$v_R(R,\varphi,t) \approx \frac{M}{4\pi\rho\alpha^3 R}\left(\frac{\alpha^2}{\beta^2} - 2\cos^2\varphi\right)\frac{1}{T_\alpha(\varphi)}\left[w'\left(t-\tau_0-\frac{T_\alpha(\varphi)}{2}-\frac{R}{\alpha}\right)-w'\left(t-\tau_0+\frac{T_\alpha(\varphi)}{2}-\frac{R}{\alpha}\right)\right]$$

-propagates with P-wave speed α, and has a “peanut shaped” radiation pattern

Far-field transverse velocity:

$$v_\varphi(R,\varphi,t) \approx \frac{M}{4\pi\rho\beta^3 R}(\sin 2\varphi)\frac{1}{T_\beta(\varphi)}\left[w'\left(t-\tau_0-\frac{T_\beta(\varphi)}{2}-\frac{R}{\beta}\right)-w'\left(t-\tau_0+\frac{T_\beta(\varphi)}{2}-\frac{R}{\beta}\right)\right]$$

-propagates with S-wave speed β, and has a sin 2φ radiation pattern

Dependence on source pulse speed v is via the two timeshift parameters:

$$\tau_0 \equiv t_0 - \frac{z_0}{v}$$

$$T_c(\varphi) \equiv \frac{h}{c}\left|\cos\varphi - \frac{c}{v}\right| \approx \begin{cases} \dfrac{h|\cos\phi|}{c} & \text{for } v >> c \\ \dfrac{h}{v} & \text{for } v << c \end{cases}$$

Resonating Line Source Solution

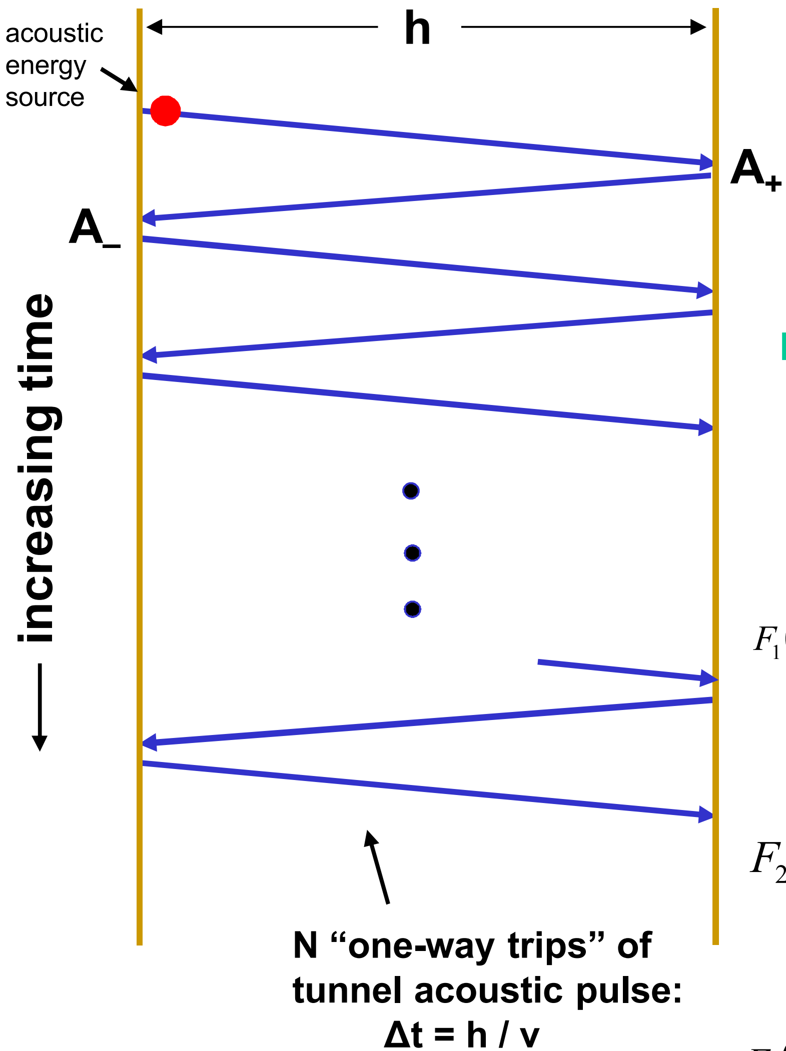

Methodology:

Utilize existing solution for a single (unidirectional) acoustic pulse propagating along tunnel, and

1) delay in time by $\Delta t = h / v$.

2) scale by tunnel end reflection coefficients A_+ and A_-.

3) sum over N "one way trips".

Tunnel resonance filter is a combination of three frequency-dependent factors:

$$H(\omega) = F_1(\omega)\, F_2(\omega) + F_3(\omega)$$

$$F_1(\omega) = \exp(-i\omega\Delta t)\left[\operatorname{sinc}\left(\frac{\omega T_c^+}{2\pi}\right)\exp\left(+i\omega\frac{\Delta t}{2}\right) + A_+ \operatorname{sinc}\left(\frac{\omega T_c^-}{2\pi}\right)\exp\left(-i\omega\frac{\Delta t}{2}\right)\right]$$

$$F_2(\omega) = \frac{1 - \left[A_+ A_- \exp(-i2\omega\Delta t)\right]^{\operatorname{int}(N/2)}}{1 - A_+ A_- \exp(-i2\omega\Delta t)}$$

The classical organ pipe filter!

$$F_3(\omega) = \left[\frac{1-(-1)^N}{1}\right](A_+ A_-)^{(N-1)/2} \operatorname{sinc}\left(\frac{\omega T_c^+}{2\pi}\right)\exp\left[-i\left(N - \frac{1}{2}\right)\omega\Delta t\right]$$

Tunnel Resonance Filter ($H = F_1 \times F_2 + F_3$)

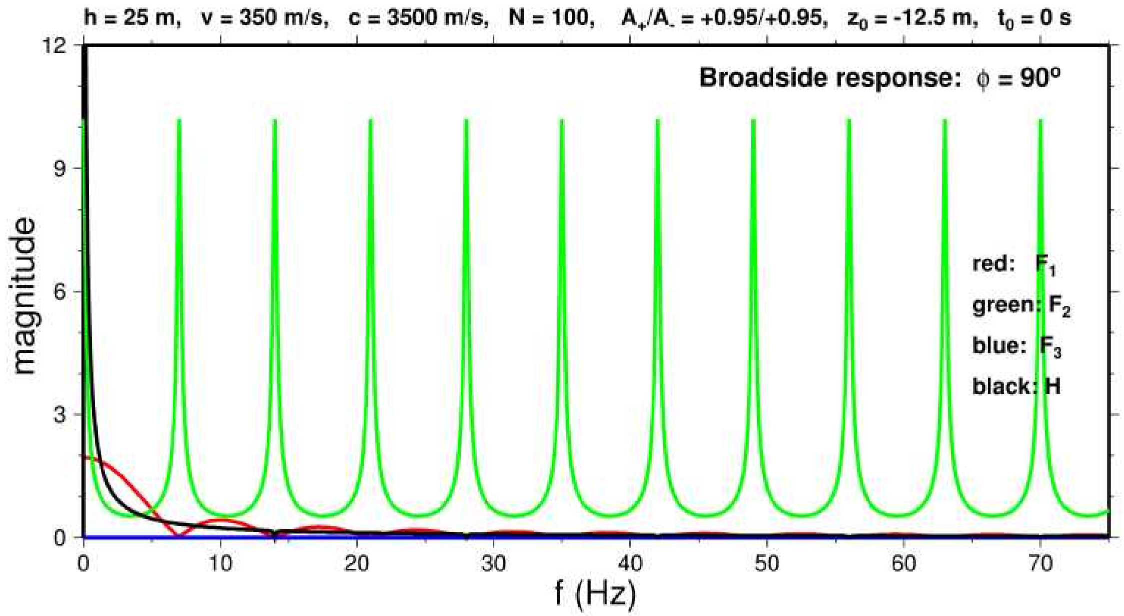

Broadside response,
Positive reflection coefficient product.

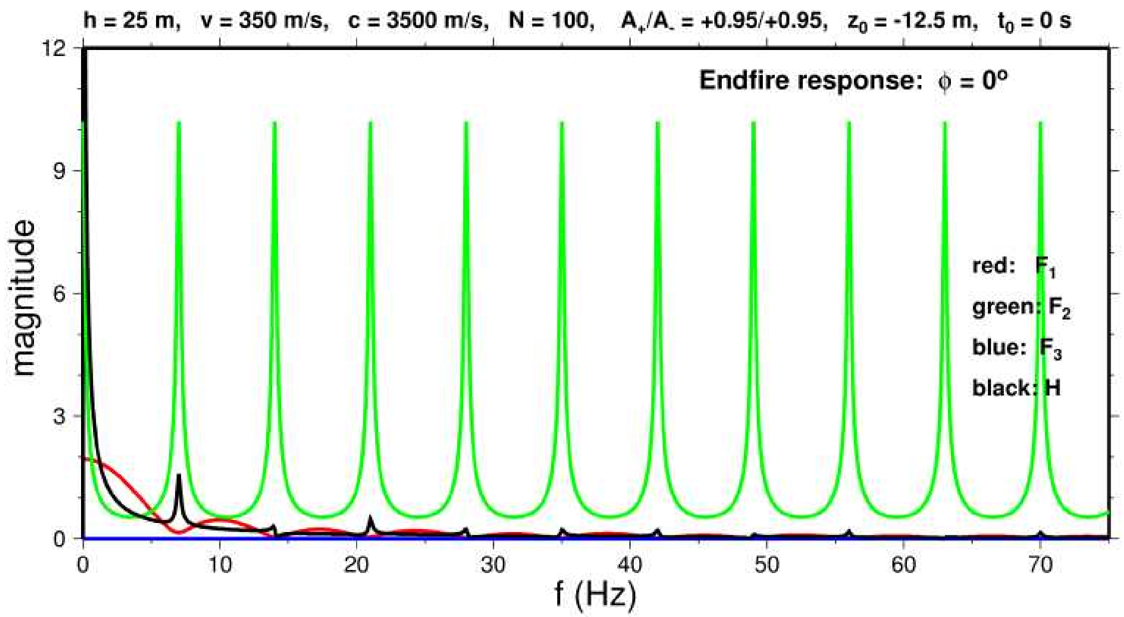

Endfire response,
Positive reflection coefficient product.

Tunnel Resonance Filter ($H = F_1 \times F_2 + F_3$)

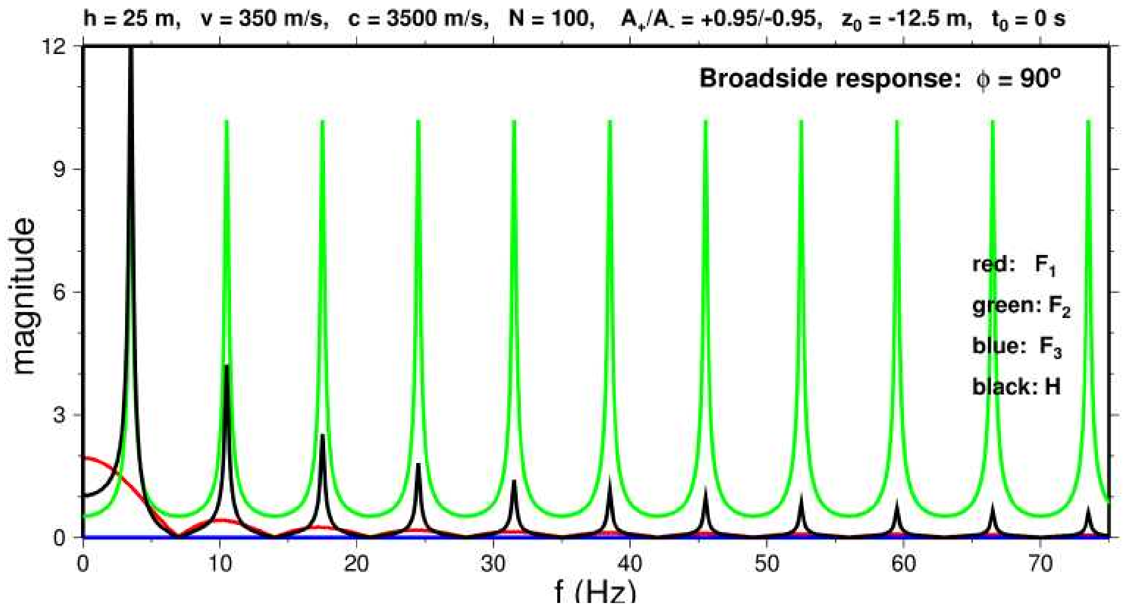

Broadside response,
Negative reflection coefficient product.

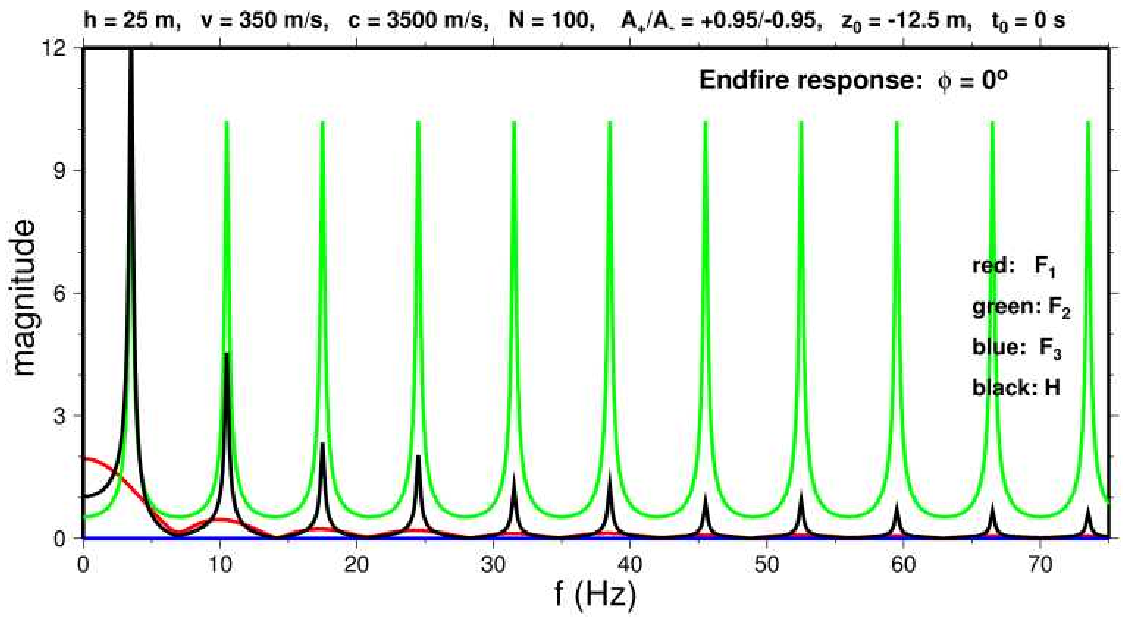

Endfire response,
Negative reflection coefficient product.

Theory vs. Numerical Experiment Comparison

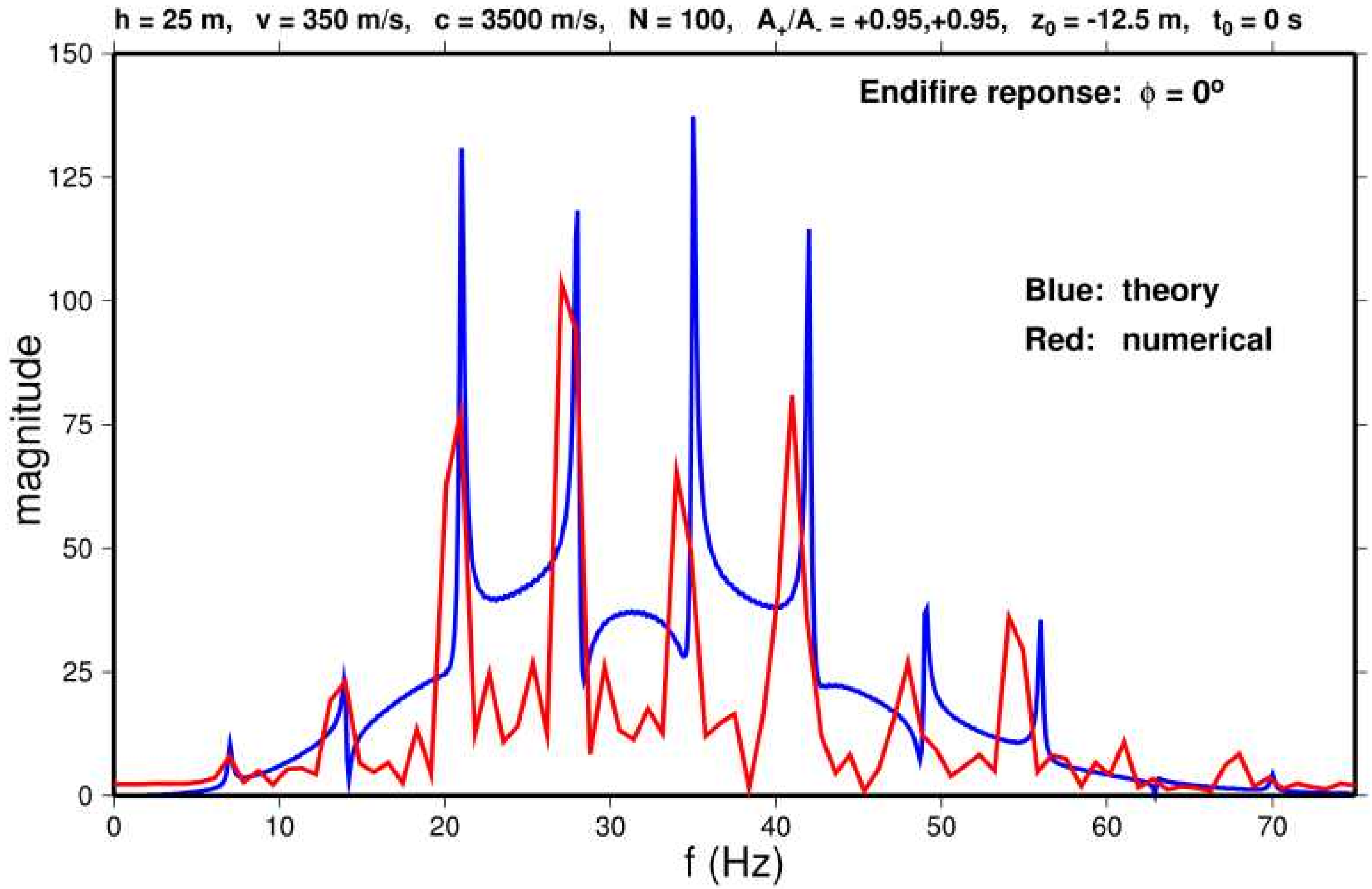

Radial particle velocity recorded at polar angle φ = 0°

Open-Ended Tunnel Model

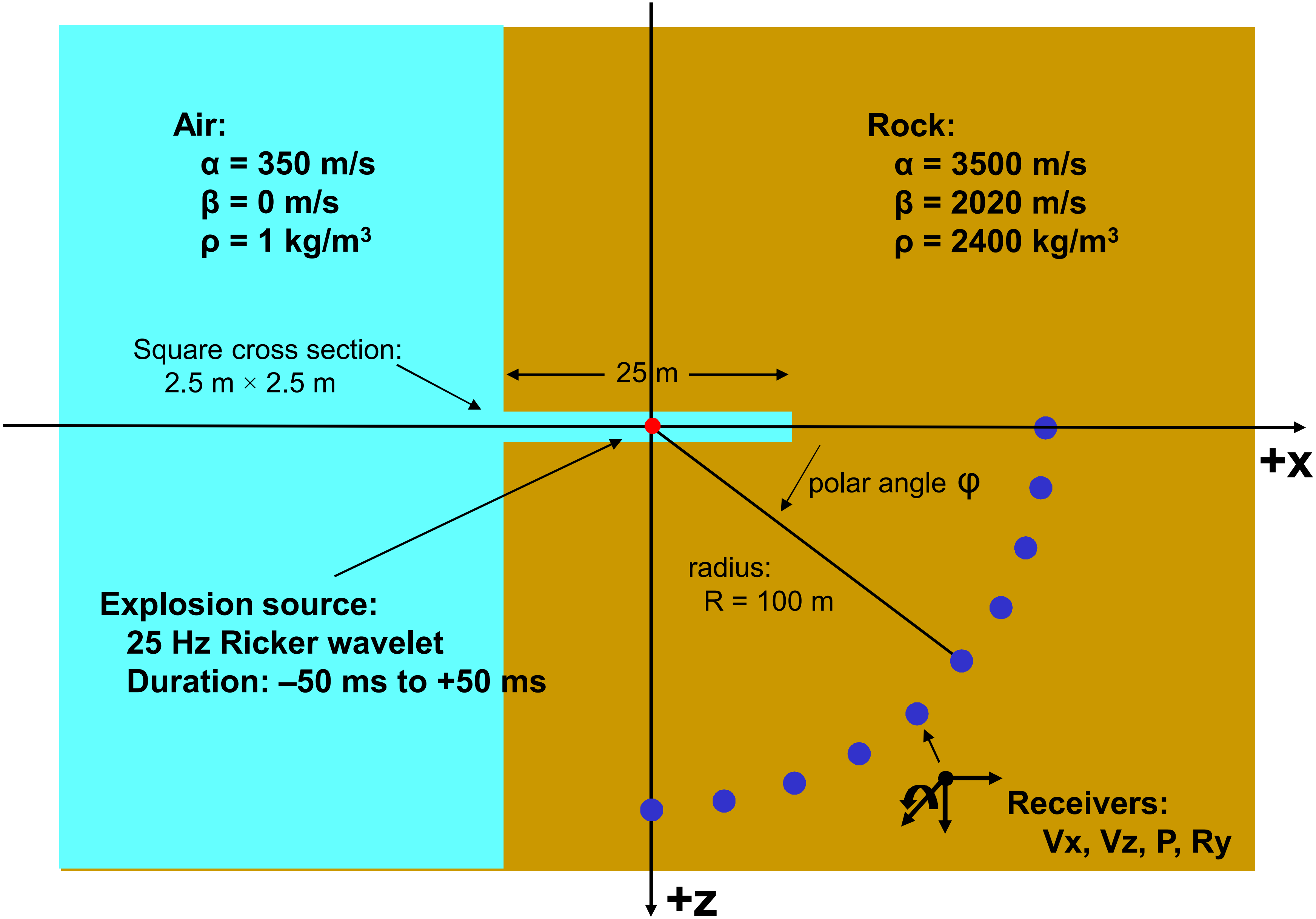

P timeslices (XZ plane at y = 0 m)

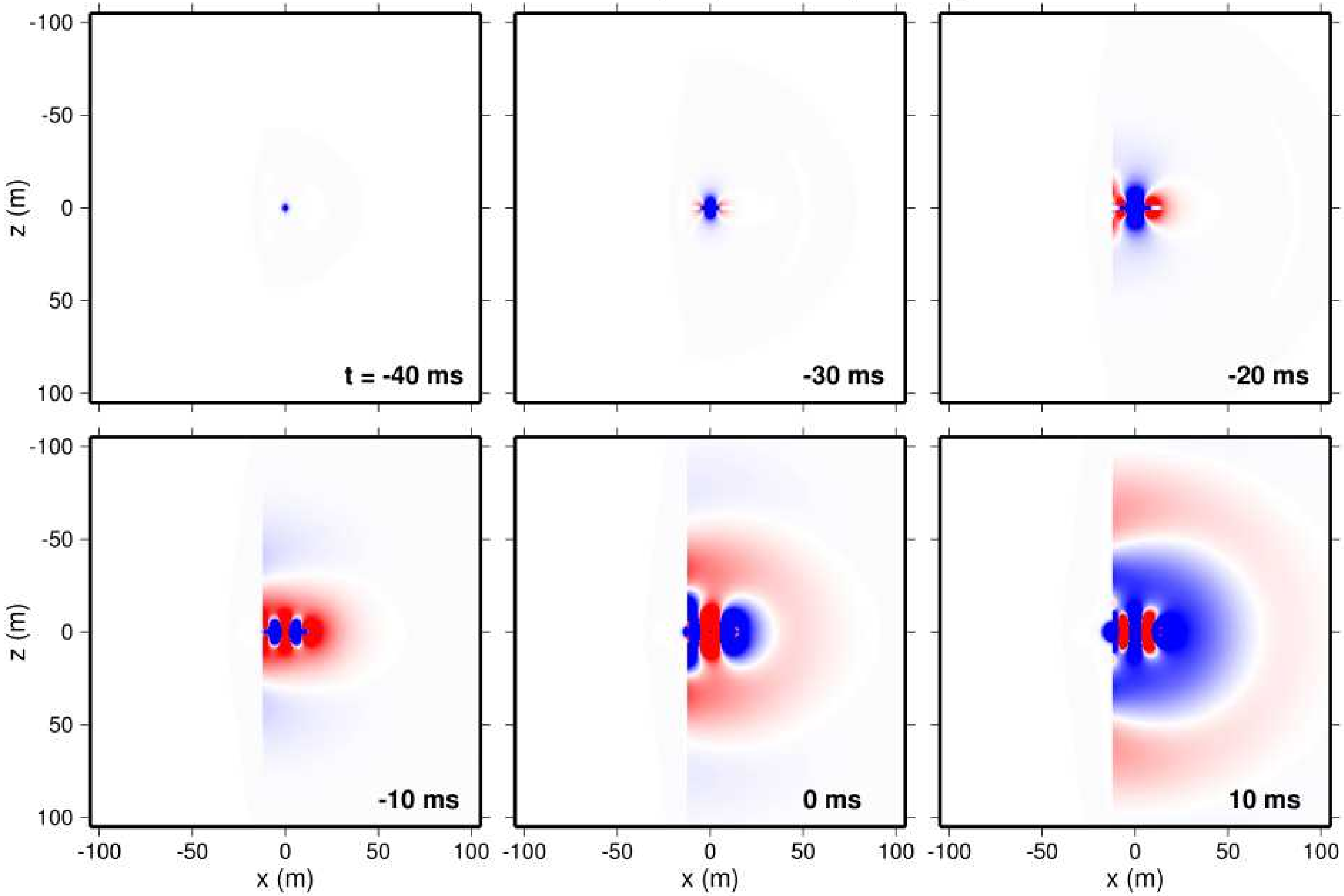

Explosion source at (0,0,0) m; 25 Hz Ricker wavelet;   Tunnel dimensions: 25 x 2.5 x 2.5 m

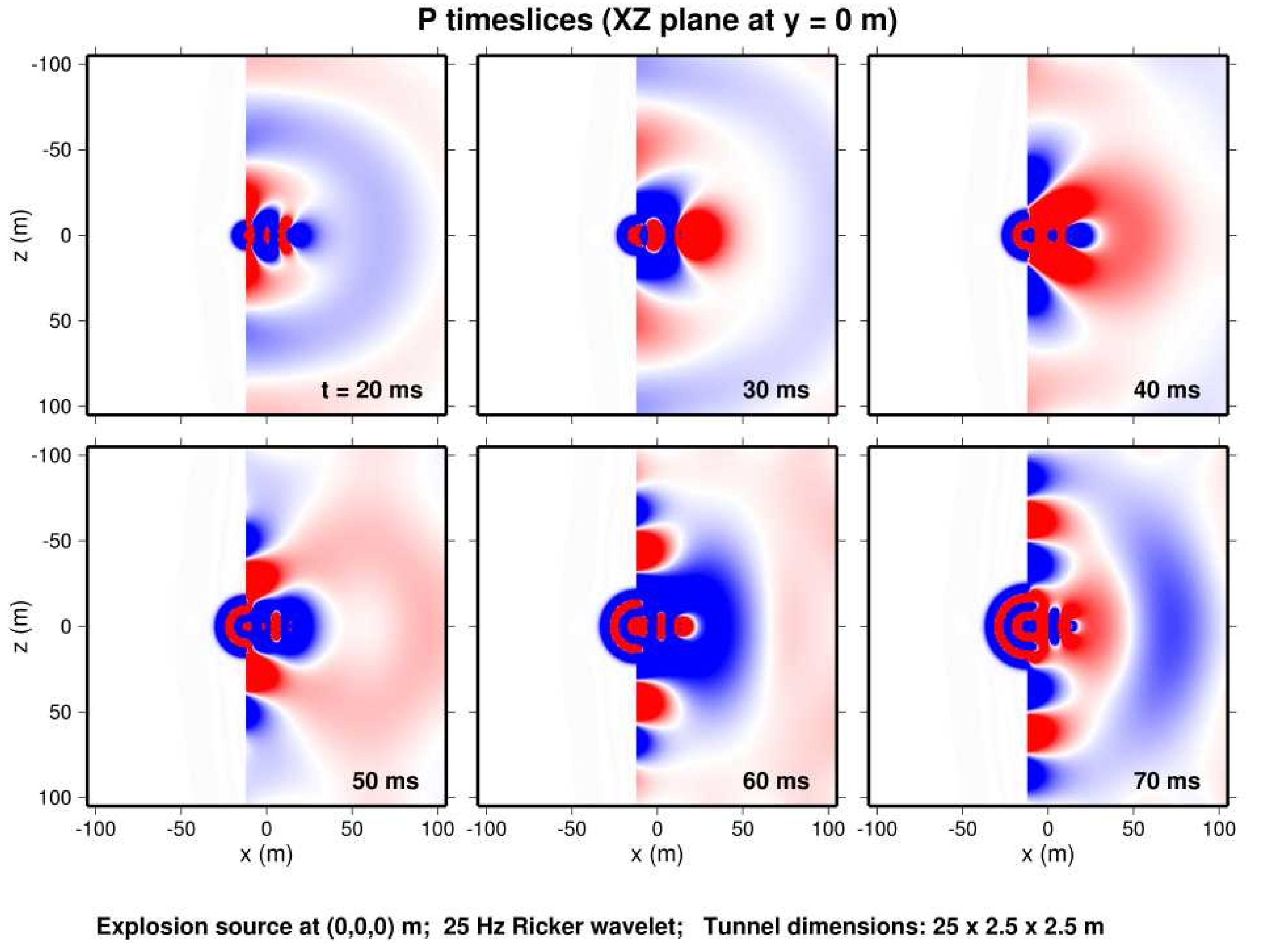
P timeslices (XZ plane at y = 0 m)
t = 20 ms
30 ms
40 ms
50 ms
60 ms
70 ms
z (m)
x (m)
-100
-50
0
50
100
Explosion source at (0,0,0) m; 25 Hz Ricker wavelet; Tunnel dimensions: 25 x 2.5 x 2.5 m

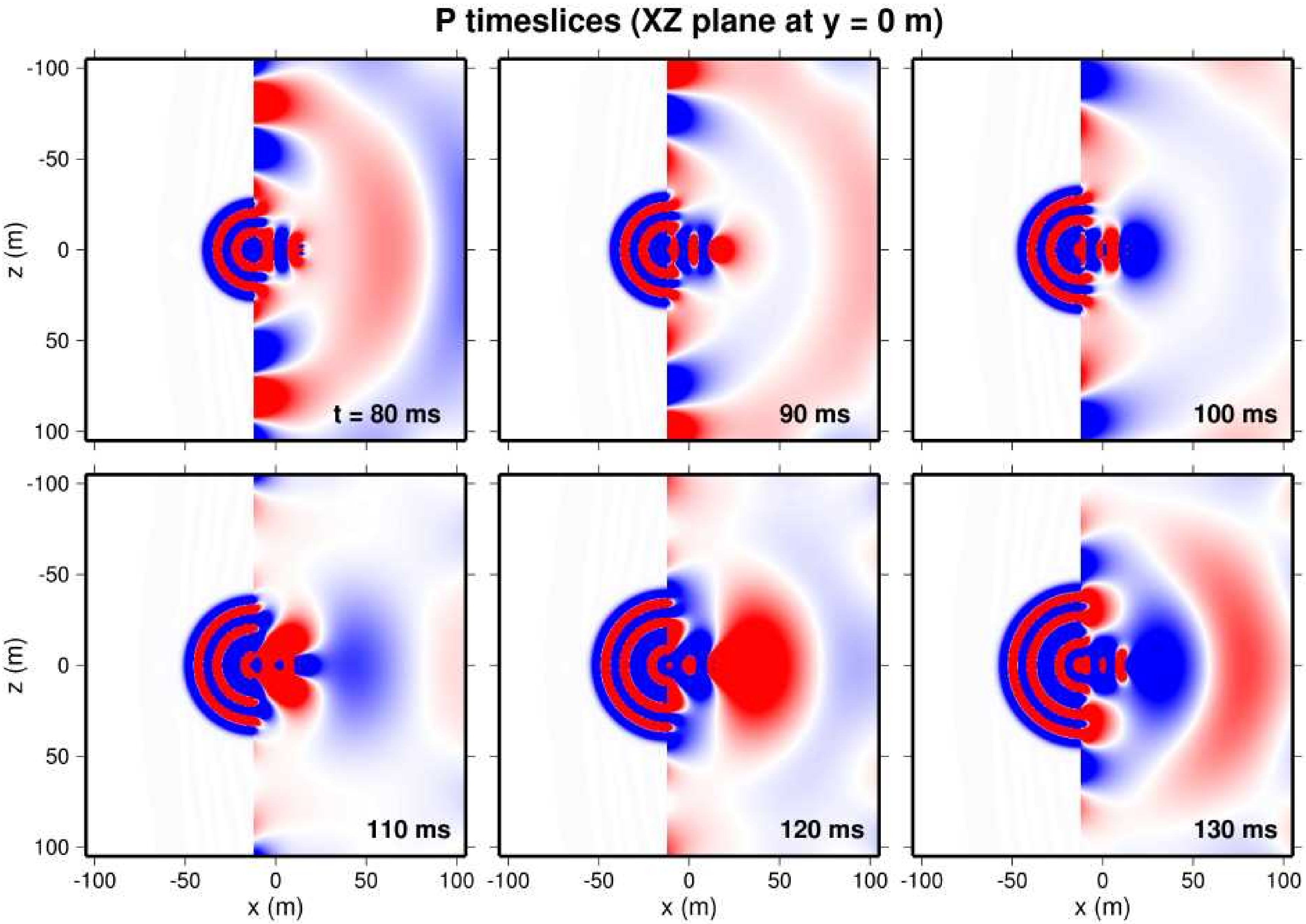

Explosion source at (0,0,0) m; 25 Hz Ricker wavelet; Tunnel dimensions: 25 x 2.5 x 2.5 m

P timeslices (XZ plane at y = 0 m)

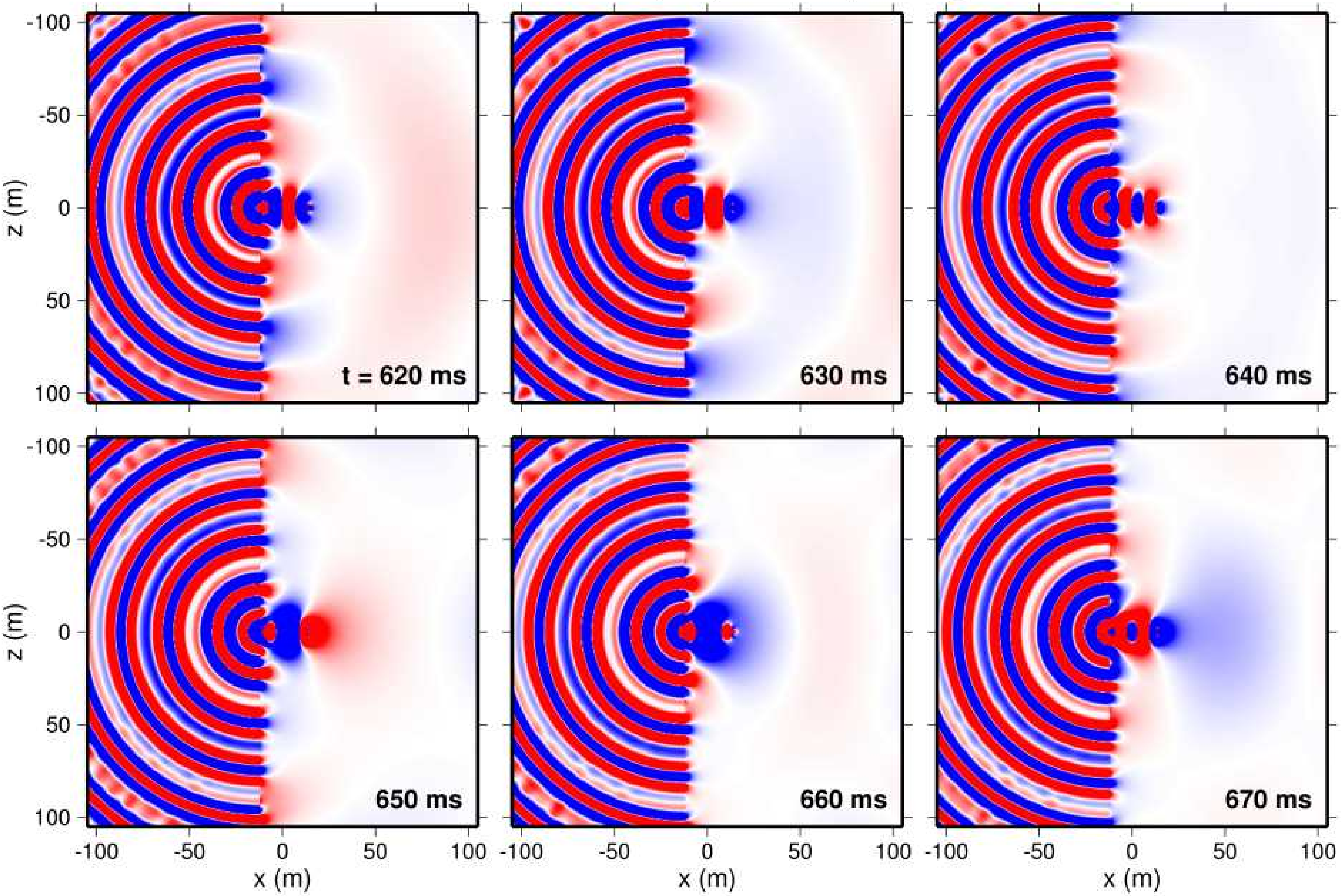

Explosion source at (0,0,0) m; 25 Hz Ricker wavelet; Tunnel dimensions: 25 x 2.5 x 2.5 m

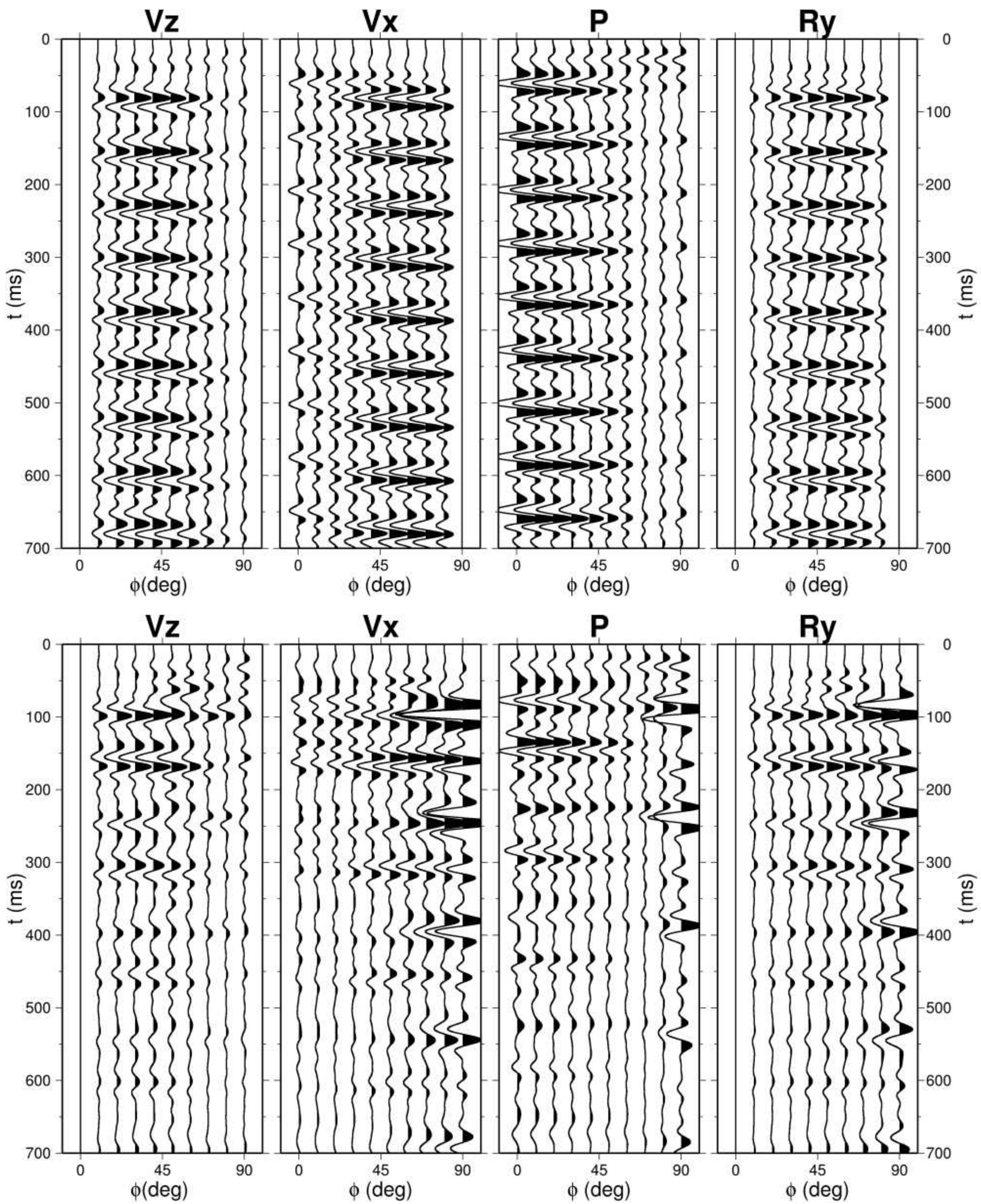

Resonant Response Comparison (Vz, Vx, P, Ry)

Enclosed tunnel

Source: (0,0,0) m
(at center of tunnel)

Left end open to air

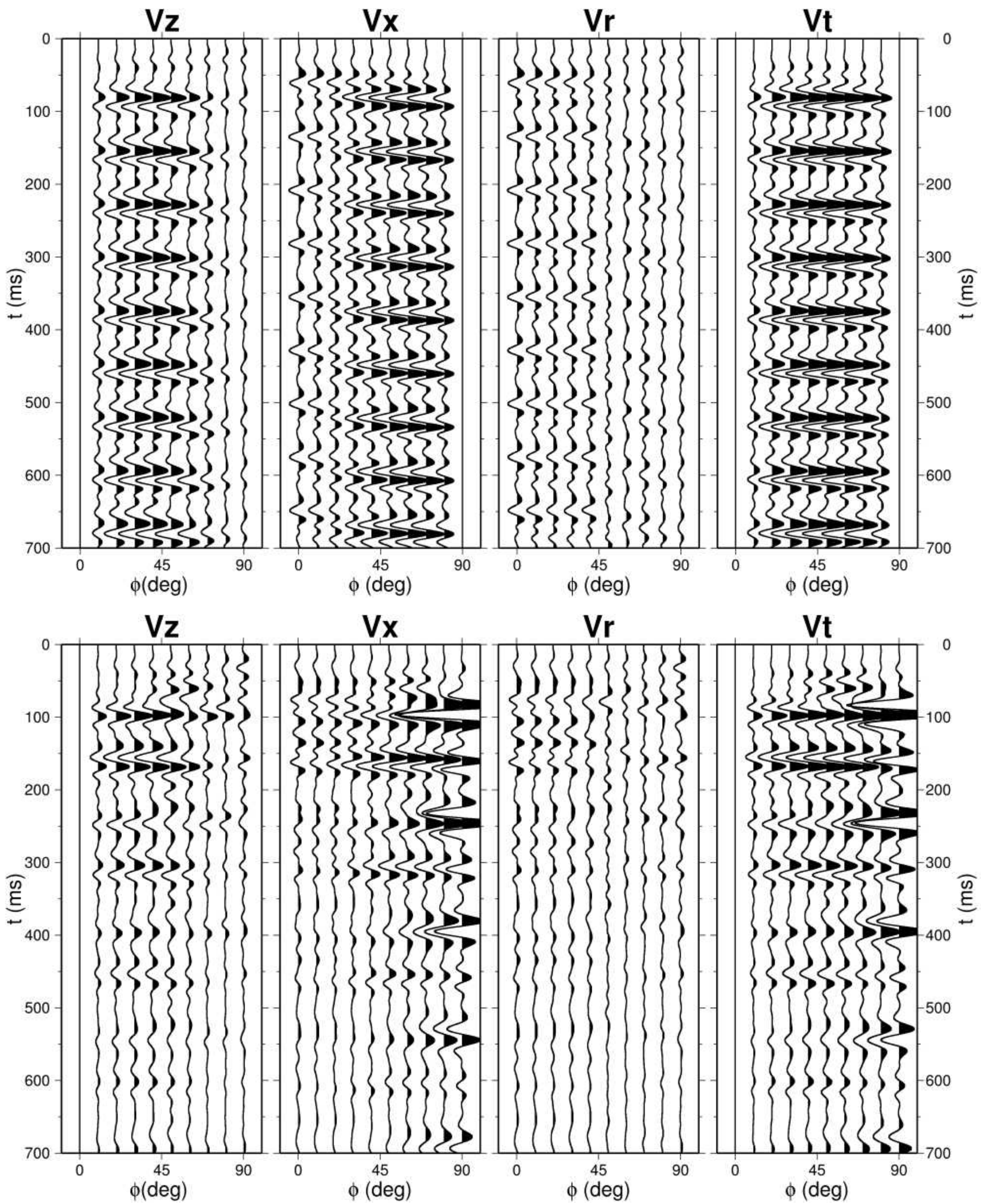

Resonant Response Comparison (Vz, Vx, Vr, Vt)

Enclosed tunnel

Source: (0,0,0) m
(at center of tunnel)

Left end open to air

Conclusions and Ongoing Work

1) Resonance behavior of enclosed/open air-filled tunnels established by numerical simulation experiments with 3D FD seismic wave propagation algorithm.

2) Resonating line-source theory requires significant improvements:
- tunnel-end reflection coefficients.
- force sources applied at tunnel endpoints.
- attenuating acoustic pulse.

3) More modeling scenarios urgently needed:
- fat tunnels.
- various cross-sectional shapes.
- non-straight tunnels.
- heterogeneity and/or topography in background model.